

**Dithienophosphole based molecular electron acceptors constructed using direct
(hetero)arylation cross-coupling methods**

Thomas A. Welsh, Audrey Laventure, Thomas Baumgartner, Gregory C. Welch*

Department of Chemistry, University of Calgary
2500 University Drive NW Calgary, AB, Canada T2N 1N4

* Corresponding Author
Email: gregory.welch@ucalgary.ca
Phone Number: 1-403-210-7603

SUPPORTING INFORMATION

Table of Contents

Materials and Methods	S3
Experimental	S5
Solution NMR Spectra	S10
Mass Spectrometry (MALDI-TOF)	S15
Elemental Analysis	S18
Optoelectronic characterization (Cyclic voltammetry/UV-Vis)	S21
Thermal properties characterization (DSC/TGA)	S30
Density Functional Theory	S33
Organic solar cells	S35
References	S39

Materials and Methods

Materials: SiliaCat® DPP-Pd was received from SiliCycle. All remaining reagents were purchased from Sigma-Aldrich. All solvents and materials purchased were used without further purification. Purification by flash column chromatography was performed using a Biotage® Isolera flash system. PTB7-Th polymer was purchased and used as is from Cal-OS. PBDB-T polymer was donated by Brilliant Matters. PDTT-BOBT polymer was donated by the research team of JC Lee at KRICT, South Korea.

Microwave-Assisted Synthesis: All microwave reactions were carried out using a Biotage® Initiator+ microwave reactor. The operational power range of the instrument is 0–400 W, using a 2.45 GHz magnetron. Pressurized air is used to cool each reaction after microwave heating.

Nuclear Magnetic Resonance (NMR): ^1H and $^{13}\text{C}\{^1\text{H}\}$ NMR spectroscopy spectra were recorded on a Bruker Avance-500 MHz spectrometer at 300 K. Chemical shifts are reported in parts per million (ppm). Multiplicities are reported as: singlet (s), doublet (d), doublet of doublets (dd), triplet (t), multiplet (m), quintet (quin), overlapping (ov), and broad (br).

High-resolution Mass Spectrometry (HRMS): High-resolution MALDI mass spectrometry measurements were performed courtesy of Jian Jun (Johnson) Li in the Chemical Instrumentation Facility at the University of Calgary. A Bruker Autoflex III Smartbeam MALDI-TOF (Na:YAG laser, 355nm), setting in positive reflective mode, was used to acquire spectra. Operation settings were all typical, e.g. laser offset 62-69; laser frequency 200Hz; and number of shots 300. The target used was Bruker MTP 384 ground steel plate target. Sample solution (~ 1 $\mu\text{g}/\text{mL}$ in dichloromethane) was mixed with matrix trans-2-[3-(4-tert-Butylphenyl)-2-methyl-2-propenylidene]malononitrile (DCTB) solution (~ 5mg/mL in methanol). Pipetted 1 μl solution above to target spot and dried in the fume hood.

Cyclic Voltammetry (CV): All electrochemical measurements were performed using a Model 1200B Series Handheld Potentiostat by CH Instruments Inc. equipped with Ag wire, Pt wire and glassy carbon electrode, as the pseudo reference, counter electrode and working electrode respectively. Glassy carbon electrodes were polished with alumina. The cyclic voltammetry experiments were performed in anhydrous dichloromethane solution with ~0.1 M tetrabutylammonium hexafluorophosphate (TBAPF₆) as the supporting electrolyte at scan rate 100 mV/s. All electrochemical solutions were purged with dry N₂ for 5 minutes to deoxygenate the system. Solution CV measurements were carried out with a small molecule concentration of ~0.5 mg/mL in dichloromethane. The ionization potentials (IP) and electron affinities (EA) were estimated by correlating the onsets ($E_{\text{oxFc}/\text{Fc}^+}$, $E_{\text{redFc}/\text{Fc}^+}$) to the normal hydrogen electrode (NHE), assuming the IP of Fc/Fc⁺ to be 4.80 eV.¹

UV-Visible Spectroscopy (UV-Vis): All absorption measurements were recorded using Agilent Technologies Cary 60 UV-Vis spectrometer at room temperature. All solution

UV-Vis experiments were run in CHCl_3 using 10 mm quartz cuvettes. Neat films of pure compounds as well as donor polymer blends were prepared by spin-coating ~ 0.2 mL from a 1 % wt/v solution (CHCl_3 or blend solvents) onto clean onto Corning glass micro slides. Prior to use, glass slides were cleaned with soap and water, acetone and isopropanol, and followed by UV/ozone treatment using a Novascan UV/ozone cleaning system.

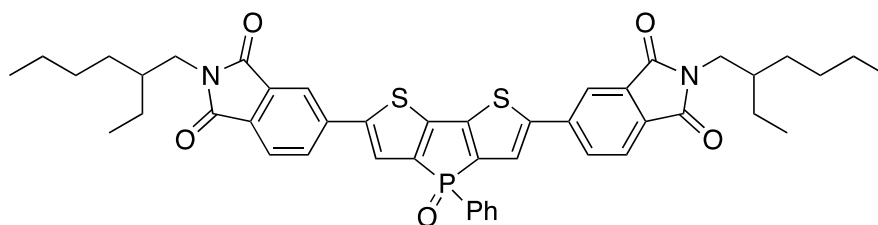
Photoluminescence (PL): All emission measurements were recorded using an Agilent Technologies Cary Eclipse fluorescence spectrophotometer at room temperature. Thin-films were prepared by spin-coating 1 wt/v% solutions from CHCl_3 or blend solvents on Corning glass micro slides. Prior to use, glass slides were cleaned with soap and water, acetone and isopropanol and followed by UV/ozone treatment using a Novascan UV/ozone cleaning system.

Density Functional Theory: Calculations were carried out using Gaussian09,² input files and results were visualized using GausView05.³ All alkyl chains were replaced with a methyl group. The B3LYP⁴⁻⁶ level of theory with 6-31G(d,p)⁷⁻¹² basis set were used for the calculations. TD-SCF¹³ calculations were performed from the optimized geometries. Single point calculations were performed on optimized structures in order to generate molecular orbitals.

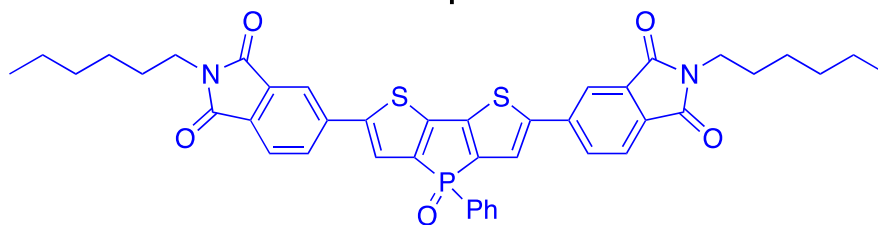
Power Conversion Efficiency (PCE) and External Quantum Efficiency (EQE): The current density-voltage (J-V) curves were measured in air by a Keithley 2420 source measure unit. The photocurrent was measured under AM 1.5 illumination at $100\text{mW}/\text{cm}^2$ under a Solar Simulator (Newport 92251A-1000). The standard silicon solar cell (Newport 91150V) was used to calibrate light intensity. EQE was measured in a QEX7 Solar Cell Spectral Response/QE/IPCE Measurement System (PV Measurement, Model QEX7, USA) with an optical lens to focus the light into an area about 0.04cm^2 , smaller than the dot cell. The silicon photodiode was used to calibration of the EQE measurement system in the wavelength range from 300 to 1100 nm.

Atomic Force Microscopy (AFM): AFM measurements were performed by using a TT2- AFM (AFM Workshop) in tapping mode and WSxM software with a 0.01-0.025 Ohm/cm Sb (n) doped Si probe with a reflective back side aluminum coating. Samples for AFM measurements were the same ones that were used to collect the respective device parameters and EQE profiles.

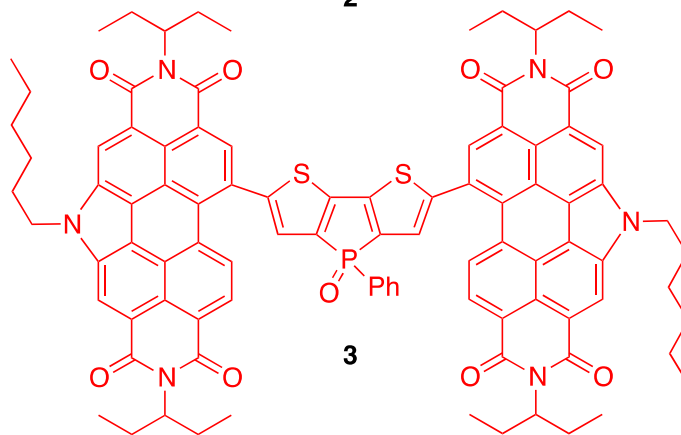
Experimental:



1



2



3

Figure S1: Final synthesized compounds.

The *N*-ethylhexyl phthalimide, *N*-hexyl phthalimide, *N*-annulated perylene diimide, and dithienophosphole building blocks were synthesized according to our previously reported literature procedures.¹⁴⁻¹⁷

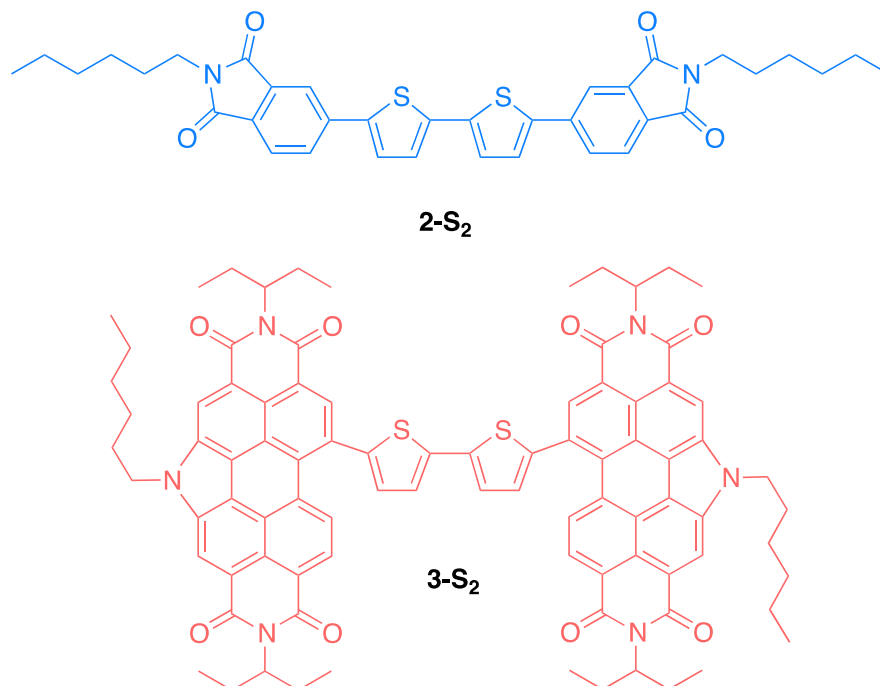
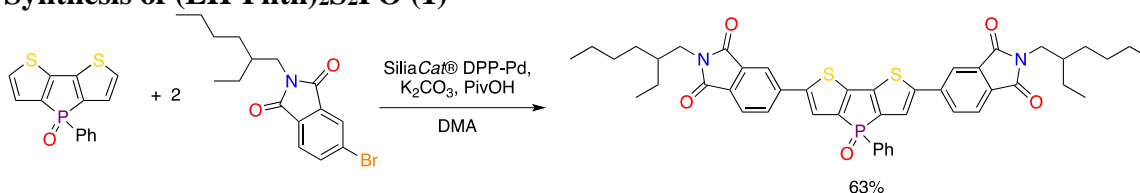


Figure S2: Phosphole-free (S₂) analogues of Compounds **2** and **3**.

Synthesis of (EH-Phth)₂S₂PO (1)



In a 5 mL pressure vial were combined dithienophosphole *P*-phenyl oxide (100 mg, 0.35 mmol, 1.0 eq.), *N*-ethylhexyl 3-bromophthalimide (235 mg, 0.70 mmol, 2.0 eq.), potassium carbonate (122 mg, 0.88 mmol, 2.5 eq.), pivalic acid (40 mol%), and SiliaCat® DPP-Pd (5 mol% Pd). The mixture was suspended with anhydrous *N,N*-dimethylacetamide, 3 mL, and the vial was sealed with a Teflon® cap under N₂ and heated at 80 °C in a LabArmor® bead bath for 16 hours. The mixture was taken up in MeOH and stirred at room temperature for 1 hour. It was then filtered through celite, rinsing with MeOH to remove the excess DMA. The orange residue left on the celite was removed by rinsing with DCM. The DCM was removed by evaporation leaving the product (175 mg, 0.22 mmol, 63%).

¹H NMR (500 MHz, CDCl₃): δ = 8.00 (s, 2H), 7.86 (m, 2H), 7.89-7.79 (m, 4H), 7.60 (m, 1H), 7.55 (d, 2H, ³J_{C-P}=2.8 Hz), 7.49 (m, 2H), 3.60 (d, 4H, ³J=7.2 Hz), 1.85 (m, 2H; CH), 1.31 (br m, 16H), 0.90 (m, 12H).

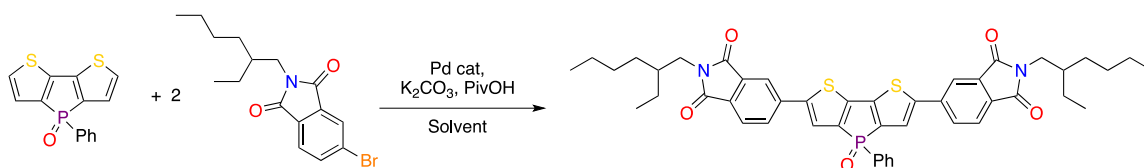
³¹P NMR (200 MHz, CDCl₃): δ = 18.5.

^{13}C NMR (125 MHz, CDCl_3 , ppm): δ 167.9, 167.9, 146.7 (d, $J_{\text{C-P}}=14.5$ Hz), 145.6 (d, $J_{\text{C-P}}=22.5$ Hz), 141.2, 140.1, 138.8, 133.5, 133.0 (d, $J_{\text{C-P}}=2.8$ Hz), 131.0 (d, $J_{\text{C-P}}=13.8$ Hz), 130.8, 130.4, 129.2 (d, $J_{\text{C-P}}=13.2$ Hz), 124.1, 123.8 (d, $J_{\text{C-P}}=14.3$ Hz), 112.0, 42.2, 38.3, 30.6, 28.5, 23.9, 23.0, 14.0, 10.4.

Tabulated aromatic peaks: 16 Tabulated aliphatic peaks: 8

MS (MALDI-TOF): m/z 803.2741 (M+H), 825.2470 (M+Na). calcd. 802.27.

Table S1: Optimization of the Reaction Conditions for 1.^a

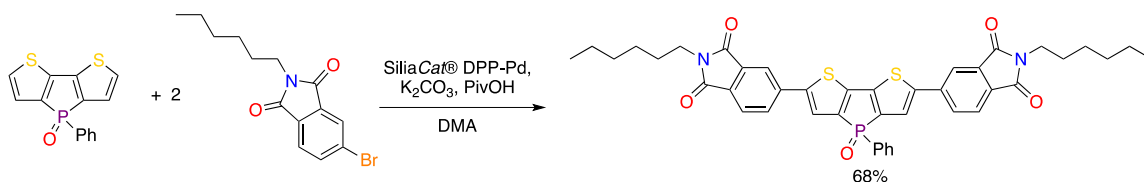


Entry	Solvent	Temp (°C)	Catalyst ^c	Phosphine ^d	Time (h)	Yield (%)
1	DMA	80	SiliaCat® DPP-Pd	————	16	63
2	1:1 Tol/H ₂ O ^b	80	SiliaCat® DPP-Pd	————	24	0
3	2-MeTHF	80	SiliaCat® DPP-Pd	————	24	<1 ^e
4	DMA	40	SiliaCat® DPP-Pd	————	24	1
5	DMA	60	SiliaCat® DPP-Pd	————	20	67
6	DMA	100	SiliaCat® DPP-Pd	————	16	39
7	DMA	80	Herrmann-Beller	P(o-anisyl) ₃	18	37
8	DMA	80	Pd(OAc) ₂	P(o-anisyl) ₃	18	22

^aReaction Conditions: S₂PO (0.17 mmol, 1.0 eq.), EH-Phth-Br (0.35 mmol, 2.0 eq.), K₂CO₃ (2-2.5 eq.), PivOH (30-40 mol%). In all cases, reagents were dissolved 1.5 mL of solvent in a 5 mL pressure vial under N₂ and heated in a LabArmor® bead bath.

^bTetrabutyl ammonium bromide (0.17 mmol, 1.0 eq.) was used as a phase transfer catalyst. ^c50 mg of SiliaCat® DPP-Pd (7 mol%), 20 mg of Herrmann-Beller (30 mol%), and 20 mg of Pd(OAc)₂ (60 mol%) were used. ^d2:1 phosphine:Pd. ^eYield was determined by ³¹P NMR spectroscopy.

Synthesis of (H-Phth)₂S₂PO (2)



In a 5 mL pressure vial were combined dithienophosphole *P*-phenyl oxide (50 mg, 0.17 mmol, 1.0 eq.), *N*-hexyl 3-bromophthalimide (108 mg, 0.35 mmol, 2.0 eq.), potassium carbonate (56 mg, 0.40 mmol, 2.3 eq.), pivalic acid (30 mol%), and SiliaCat® DPP-Pd (7

mol% Pd). The mixture was suspended with anhydrous *N,N'*-dimethylacetamide, 1.5 mL, and the vial was sealed with a Teflon® cap under N₂ and heated at 60 °C in a LabArmor® bead bath for 24 hours. The mixture was taken up in MeOH and stirred at room temperature for 1 hour. It was then filtered through celite, rinsing with MeOH to remove the excess DMA. The orange residue left on the celite was removed by rinsing with DCM. The DCM was removed by evaporation leaving the product (88 mg, 0.12 mmol, 68%).

¹H NMR (500 MHz, CDCl₃): δ = 8.00 (s, 2H), 7.86 (m, 2H), 7.89-7.79 (m, 4H), 7.60 (m, 1H), 7.55 (d, 2H, ³J_{C-P}=2.7 Hz), 7.49 (m, 2H), 3.59 (t, 4H, ³J=7.3 Hz), 1.67 (pent, 4H, ³J=6.4 Hz), 1.31 (br m, 12H), 0.88 (t, 6H, ³J=6.9 Hz).

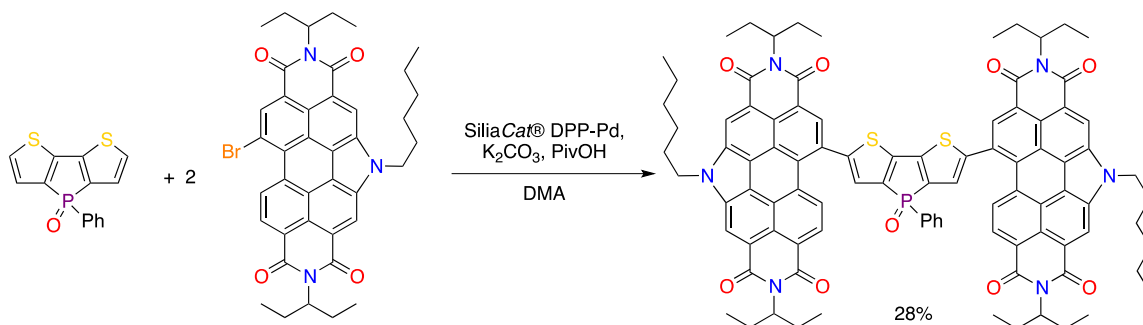
³¹P NMR (200 MHz, CDCl₃): δ = 18.3.

¹³C NMR (125 MHz, CDCl₃, ppm): δ 167.9, 167.8, 146.8 (d, J_{C-P}=14.3 Hz), 145.7 (J_{C-P}=22.6 Hz), 141.2, 140.3, 138.9, 133.6, 133.2 (d, J_{C-P}=2.3 Hz), 131.2, 131.0 (d, J_{C-P}=11.4 Hz), 130.5, 129.4 (d, J_{C-P}=13.2 Hz), 124.2, 124.0 (d, J_{C-P}=14.3 Hz), 120.1, 38.4, 31.5, 28.7, 26.7, 22.7, 14.2.

Tabulated aromatic peaks: 16 Tabulated aliphatic peaks: 6

MS (MALDI-TOF): *m/z* 747.2132 (M+H), 769.1765 (M+Na). calcd. 746.20.

Synthesis of (H-PDI)₂S₂PO (3)



In a 5 mL pressure vial were combined dithienophosphole *P*-phenyl oxide (50 mg, 0.17 mmol, 1.0 eq.), 11-bromo-5-hexyl-2,8-bis(1-ethylpropyl)perylene diimide (246 mg, 0.35 mmol, 2.0 eq.), potassium carbonate (58 mg, 0.42 mmol, 2.4 eq.), pivalic acid (46 mol%), and SiliaCat® DPP-Pd (7 mol% Pd). The mixture was suspended in anhydrous *N,N'*-dimethylacetamide, 3 mL, and the vial was sealed with a Teflon® cap under N₂ and heated at 80 °C in a LabArmor® bead bath for 24 hours until the PDI was gone by TLC. After 24 hours the mixture was taken up in MeOH and stirred for one hour. The mixture was then filtered through a celite, rinsing with MeOH to remove excess DMA and mono-substituted product. Dichloromethane was then used to remove the product. This solution was filtered through a short silica plug, rinsing with DCM to remove a fluorescent impurity. When the fluorescent impurity was no longer visible the product was removed by rinsing with 10:1 DCM/NEt₃. The solution was concentrated and the product was precipitated with MeOH and isolated by vacuum filtration (73 mg, 0.048 mmol, 28%).

An alternative synthesis involved microwave heating. The same amounts of reagents were combined in a 2 mL pressure vial and suspended in anhydrous *N,N'*-dimethylacetamide, 1.5 mL. The vial was sealed, purged with N₂, and heated at 80 °C in the microwave with monitoring by TLC after 1, 2, and 4 hours of reaction time. After 4 hours TLC indicated the absence of dithienophosphole *P*-phenyl oxide and the reaction mixture was taken up in MeOH and stirred for one hour. The mixture was then filtered through celite, rinsing with MeOH to remove excess DMA and mono-substituted product. Dichloromethane was then used to remove the product. This solution was then concentrated and solid was precipitated with MeOH and isolated via vacuum filtration. The solid was purified via column chromatography, eluting with a hexanes to ethyl acetate gradient (129 mg, 0.084 mmol, 49%).

¹H NMR (500 MHz, CDCl₃, ppm): δ 9.11 (s, 2H), 9.07 (s, 2H), 8.87 (br s, 2H), 8.75-8.50 (br m, 4H), 8.07 (br m, 2H), 7.78 (br m, 1H), 7.73 (br m, 2H), 7.60 (d, 2H, ³*J*=2.0 Hz), 5.22 (m, 4H), 4.94 (t, 4H, ³*J*=7.2 Hz), 2.36 (m, 8H), 2.24 (pent, 4H, ³*J*=7.4 Hz), 2.01 (m, 8H), 1.52-1.25 (m, 12H), 0.98 (t, 12H, ³*J*=7.4 Hz), 0.97 (t, 12H, ³*J*=7.4 Hz), 0.87 (t, 6H, ³*J*=7.2 Hz).

³¹P NMR (200 MHz, CDCl₃, ppm): δ 18.5.

¹³C NMR (125 MHz, CDCl₃, ppm): δ 147.1 (d, *J*_{C-P}=22.7 Hz), 146.8 (d, *J*_{C-P}=14.7 Hz), 140.9, 140.0, 135.2, 135.1, 133.5, 132.7, 132.1 (d, *J*_{C-P}=5.1 Hz), 131.0 (d, *J*_{C-P}=11.3 Hz), 129.7 (d, *J*_{C-P}=13.1 Hz), 129.5, 126.4, 126.3, 125.2, 125.0, 123.2 (d, *J*_{C-P}=10.7 Hz), 120.0, 119.8, 58.0, 57.9, 47.1, 31.7, 31.5, 29.8, 27.0, 25.3, 22.6, 14.1, 11.6, 11.5.

Tabulated aromatic peaks: 19 Tabulated aliphatic peaks: 12

MS (MALDI-TOF): *m/z* 1537.5549, 1561.5606 (M+Na). calcd. 1538.57.

NMR Spectra

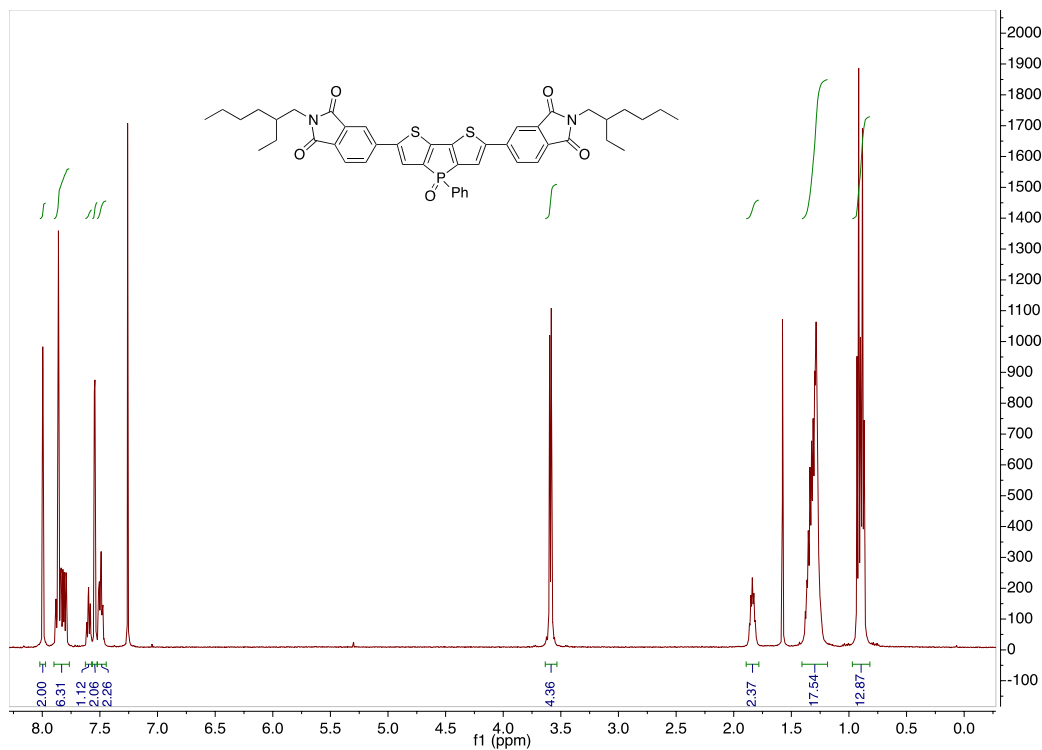


Figure S3: ¹H NMR Spectrum of (EH-Phth)₂S₂PO (1) in CDCl₃.

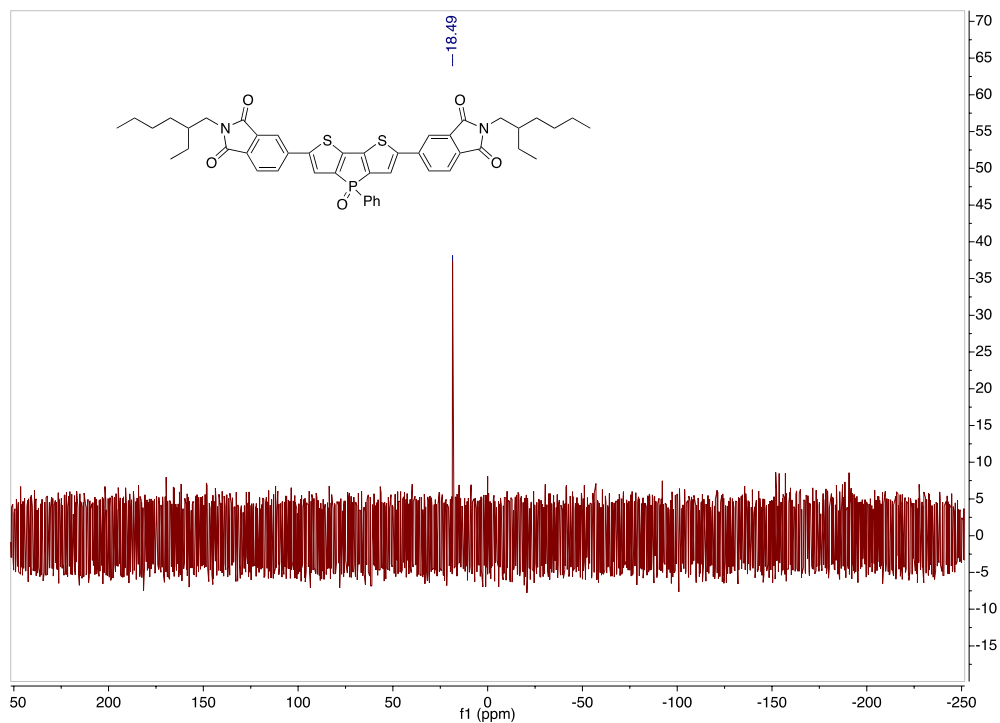


Figure S4: ³¹P NMR Spectrum of (EH-Phth)₂S₂PO (1) in CDCl₃.

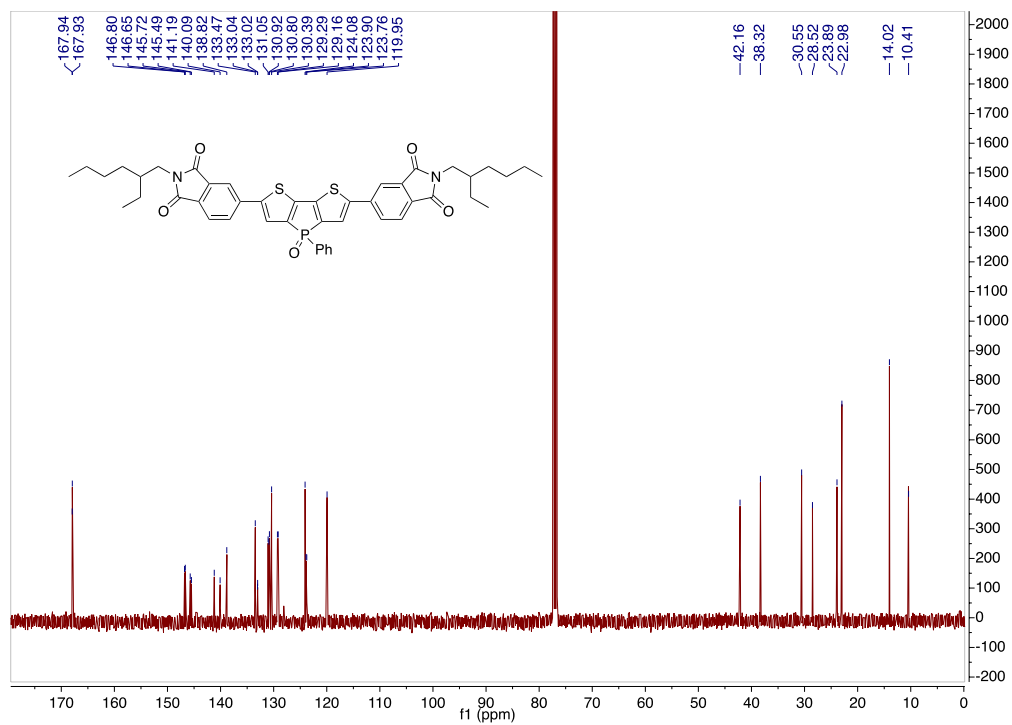


Figure S5: ¹³C NMR Spectrum of (EH-Phth)₂S₂PO (1) in CDCl₃.

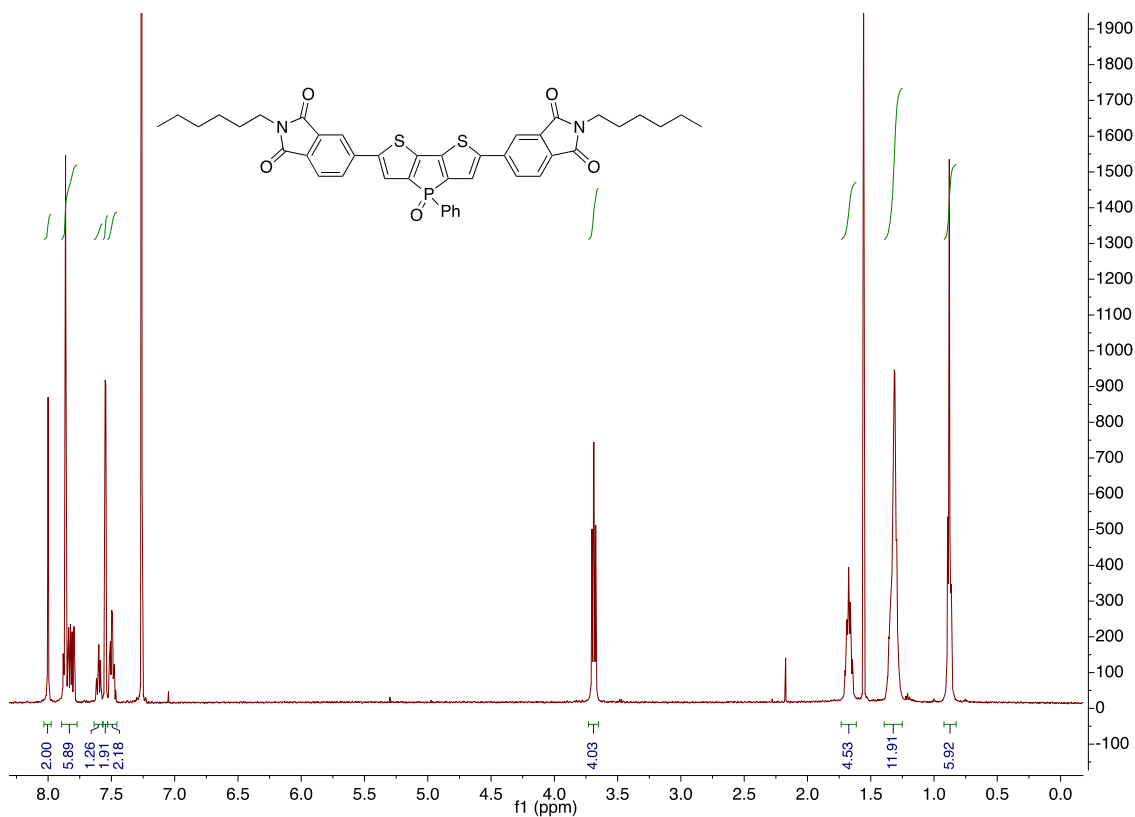


Figure S6: ¹H NMR Spectrum of (H-Phth)₂S₂PO (2) in CDCl₃.

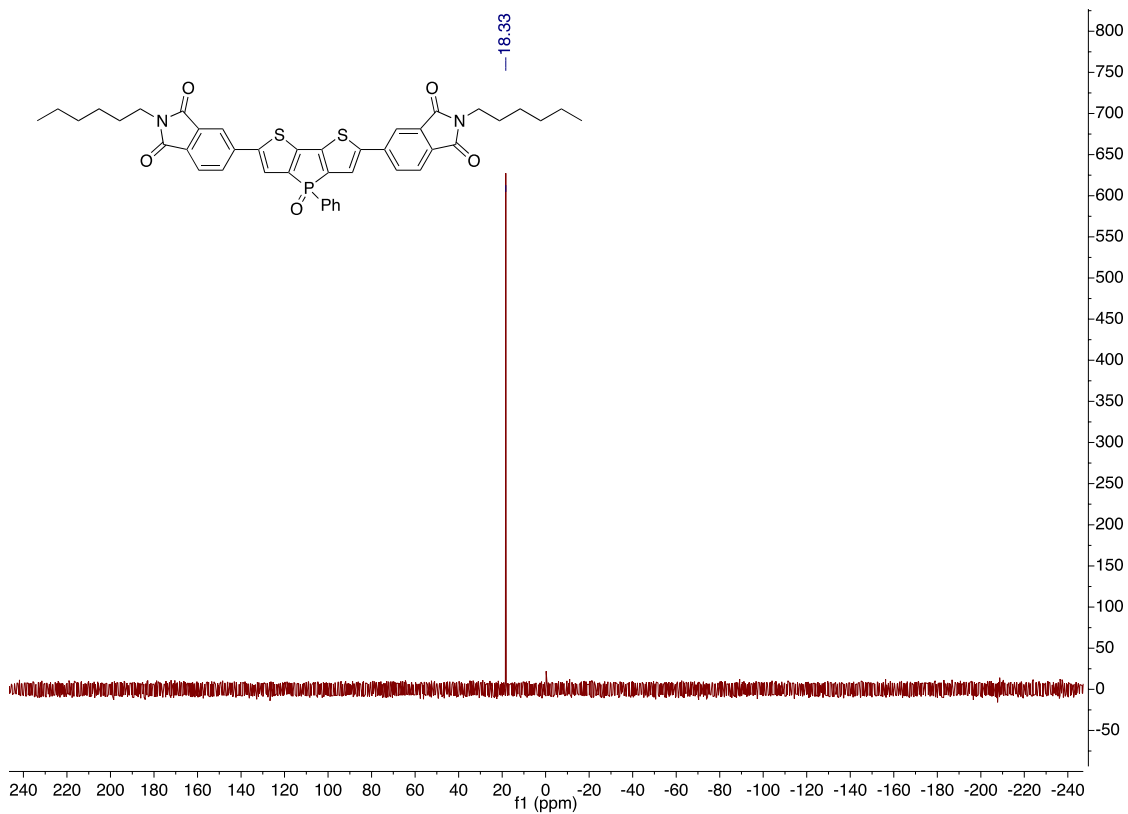


Figure S7: ³¹P NMR Spectrum of (H-Phth)₂S₂PO (2) in CDCl₃.

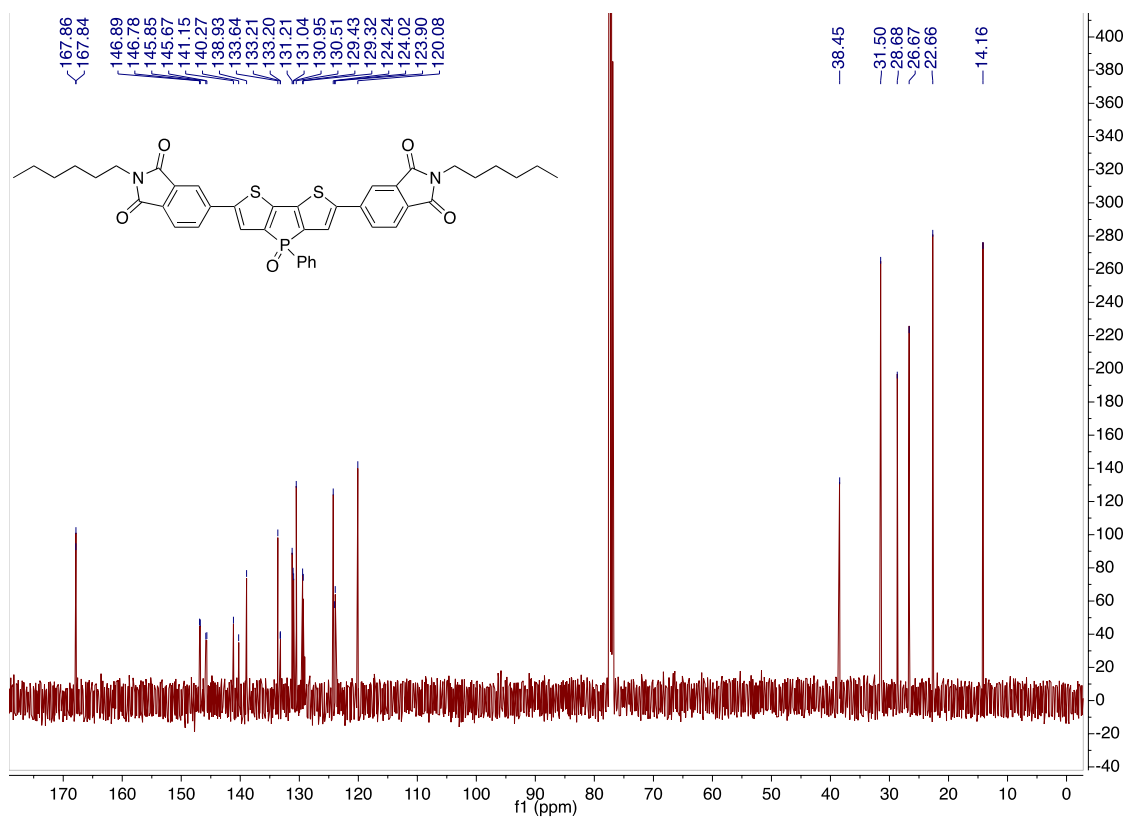


Figure S8: ¹³C NMR Spectrum of (H-Phth)₂S₂PO (2) in CDCl₃.

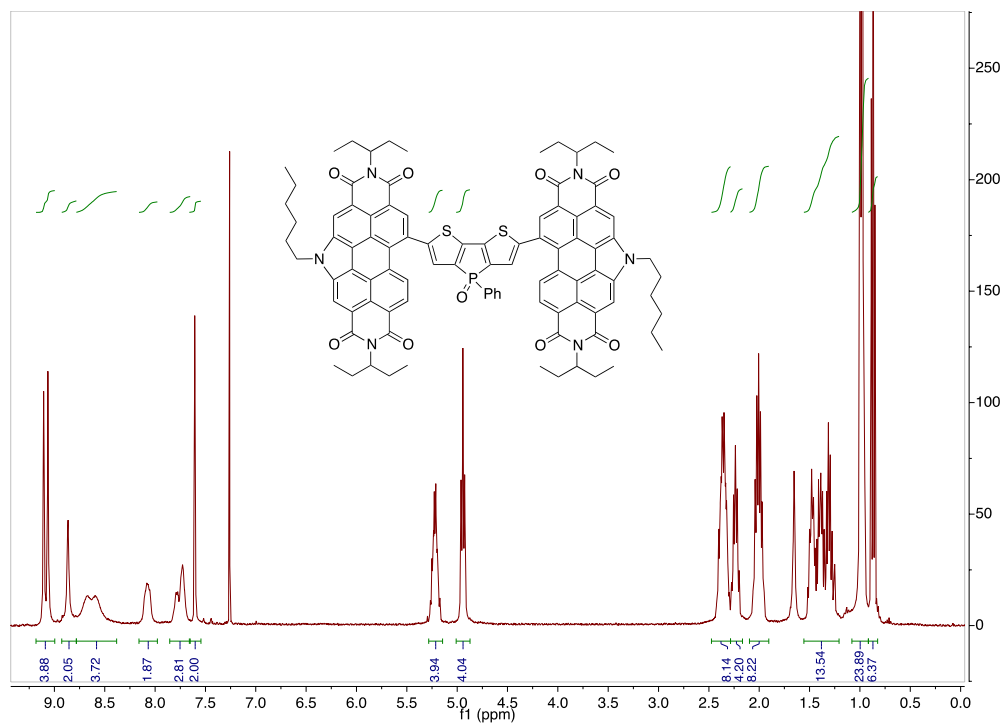


Figure S9: ¹H NMR Spectrum of (H-PDI)₂S₂PO (3) in CDCl₃.

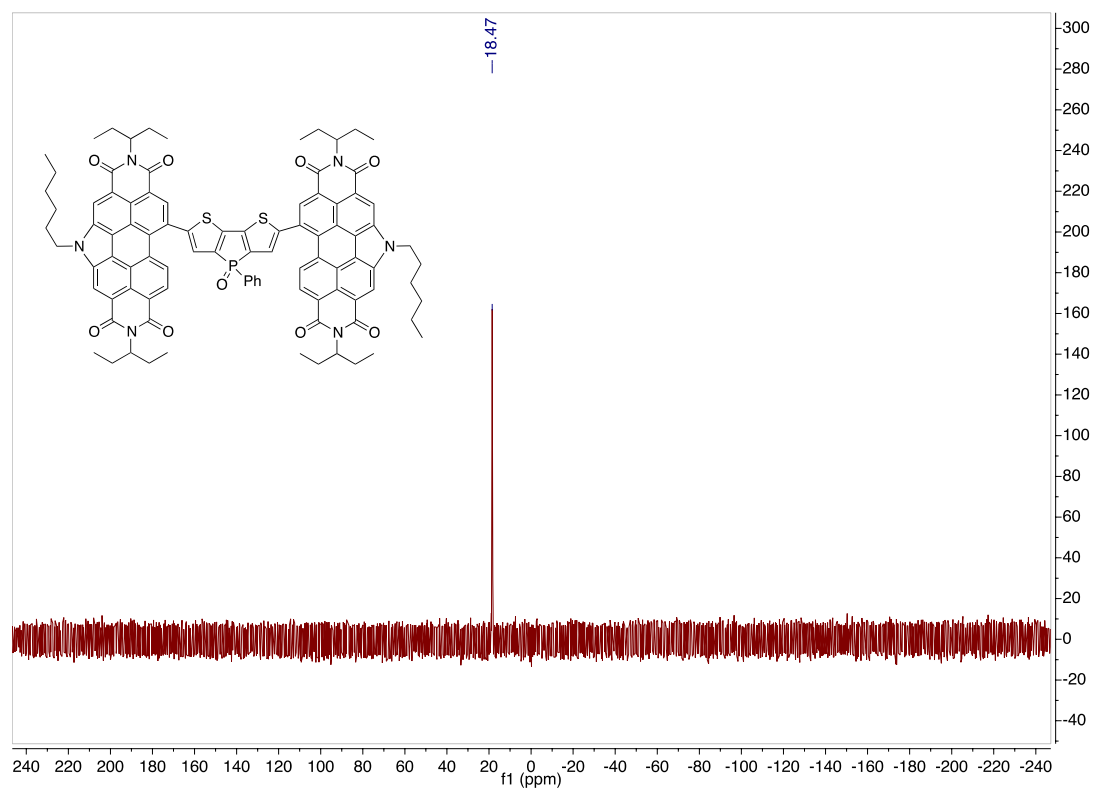


Figure S10: ³¹P NMR Spectrum of (H-PDI)₂S₂PO (3) in CDCl₃.

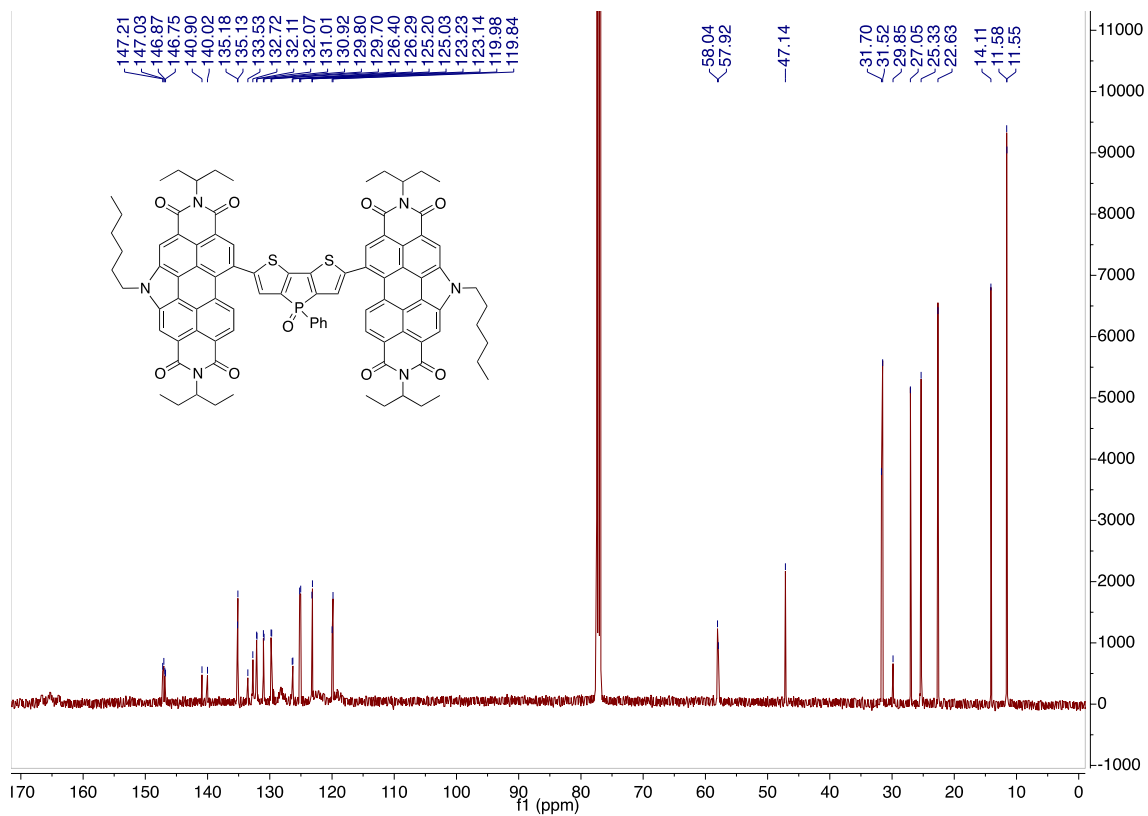


Figure S11: ¹³C NMR Spectrum of (H-PDI)₂S₂PO (3) in CDCl₃.

Mass Spectra (MALDI-TOF)

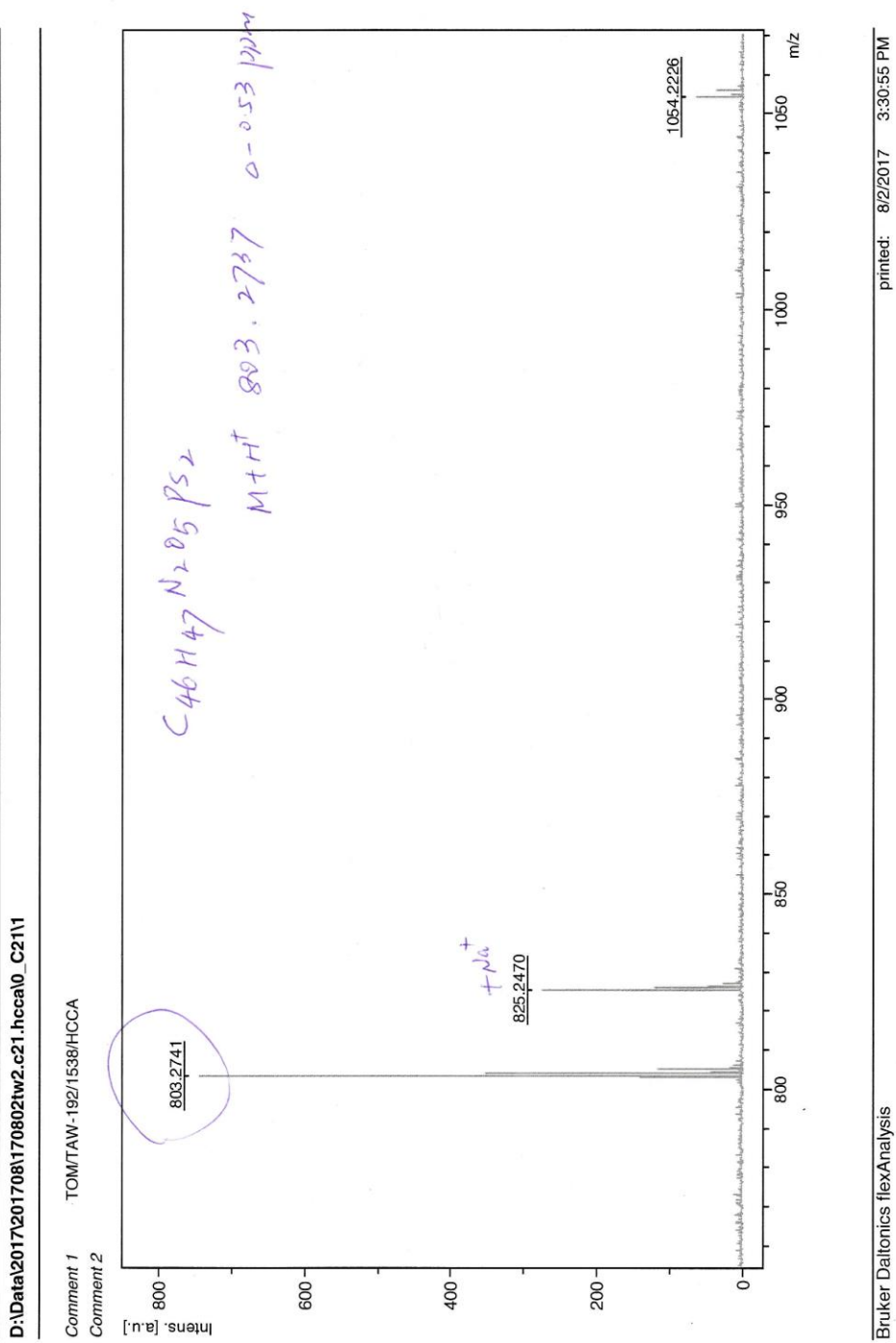
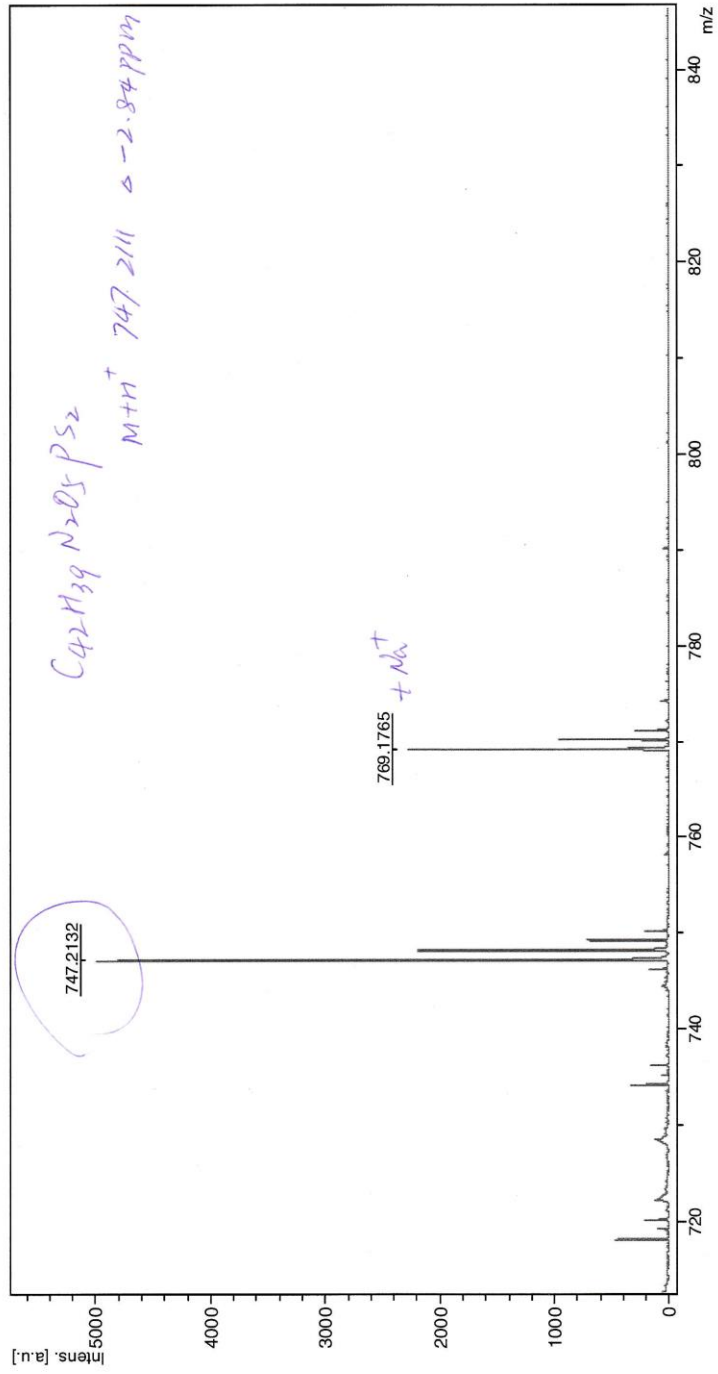


Figure S12: MALDI-TOF of (EH-Phth)₂S₂PO (1).

D:\Data\2017\10\GW171004TW1.10.HCCA0_1101

Comment 1 TOMITAW211746/HCCA
Comment 2



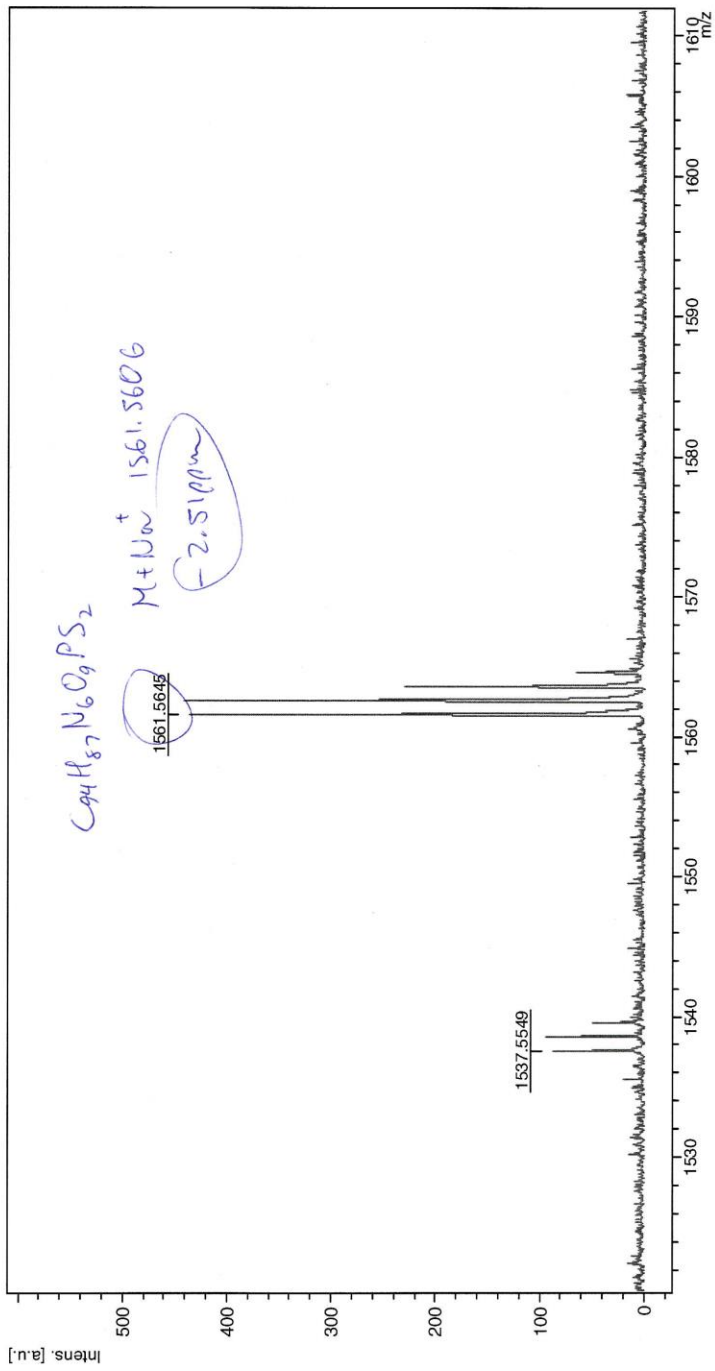
Bruker Daltonics flexAnalysis

printed: 10/4/2017 1:28:57 PM

Figure S13: MALDI-TOF of (H-Phth)₂S₂PO (2).

D:\Data\2017\08\170802\TW1_A21.HCCA\0_A211

Comment 1 TOM/TAW-194/1538/HCCA
Comment 2



Bruker Daltonics flexAnalysis

printed: 8/2/2017 3:18:43 PM

Figure S14: MALDI-TOF of (H-PDI)₂S₂PO (3).

Elemental Analysis

University of Calgary
Department of Chemistry EA Date: 12/13/2017

Name:	THOMAS	Group:	GW
Sample:	TAW192-1	Weight (mg):	1.276
%C (Actual):	68.63	%C (Theoretical):	68.81
%H (Actual):	5.84	%H (Theoretical):	5.90
%N (Actual):	3.43	%N (Theoretical):	3.49

University of Calgary
Department of Chemistry EA Date: 12/13/2017

Name:	THOMAS	Group:	GW
Sample:	TAW192-2	Weight (mg):	1.428
%C (Actual):	68.74	%C (Theoretical):	68.81
%H (Actual):	5.80	%H (Theoretical):	5.90
%N (Actual):	3.44	%N (Theoretical):	3.49

Figure S15: Elemental analysis results of (EH-Phth)₂S₂PO (1).

University of Calgary
Department of Chemistry EA Date: 12/13/2017

Name:	THOMAS	Group:	GW
Sample:	TAW211-1	Weight (mg):	0.957
%C (Actual):	67.27	%C (Theoretical):	67.54
%H (Actual):	5.45	%H (Theoretical):	5.26
%N (Actual):	3.63	%N (Theoretical):	3.75

University of Calgary
Department of Chemistry EA Date: 12/13/2017

Name:	THOMAS	Group:	GW
Sample:	TAW211-2	Weight (mg):	1.12
%C (Actual):	67.47	%C (Theoretical):	67.54
%H (Actual):	5.36	%H (Theoretical):	5.26
%N (Actual):	3.63	%N (Theoretical):	3.75

Figure S16: Elemental analysis results of (H-Phth)₂S₂PO (2).

University of Calgary
Department of Chemistry EA Date: 12/13/2017

Name:	THOMAS	Group:	GW
Sample:	TAW194-1	Weight (mg):	1.112
%C (Actual):	70.41	%C (Theoretical):	73.32
%H (Actual):	5.67	%H (Theoretical):	5.69
%N (Actual):	5.11	%N (Theoretical):	5.46

University of Calgary
Department of Chemistry EA Date: 12/13/2017

Name:	THOMAS	Group:	GW
Sample:	TAW194-2	Weight (mg):	1.209
%C (Actual):	70.44	%C (Theoretical):	73.32
%H (Actual):	5.61	%H (Theoretical):	5.69
%N (Actual):	5.12	%N (Theoretical):	5.46

Figure S17: Elemental analysis results of (H-PDI)₂S₂PO (**3**). Note: %C results are lower than theoretical due to incomplete combustion of perylene diimide units.

Optoelectronic Characterization (Cyclic Voltammetry/UV-Vis)

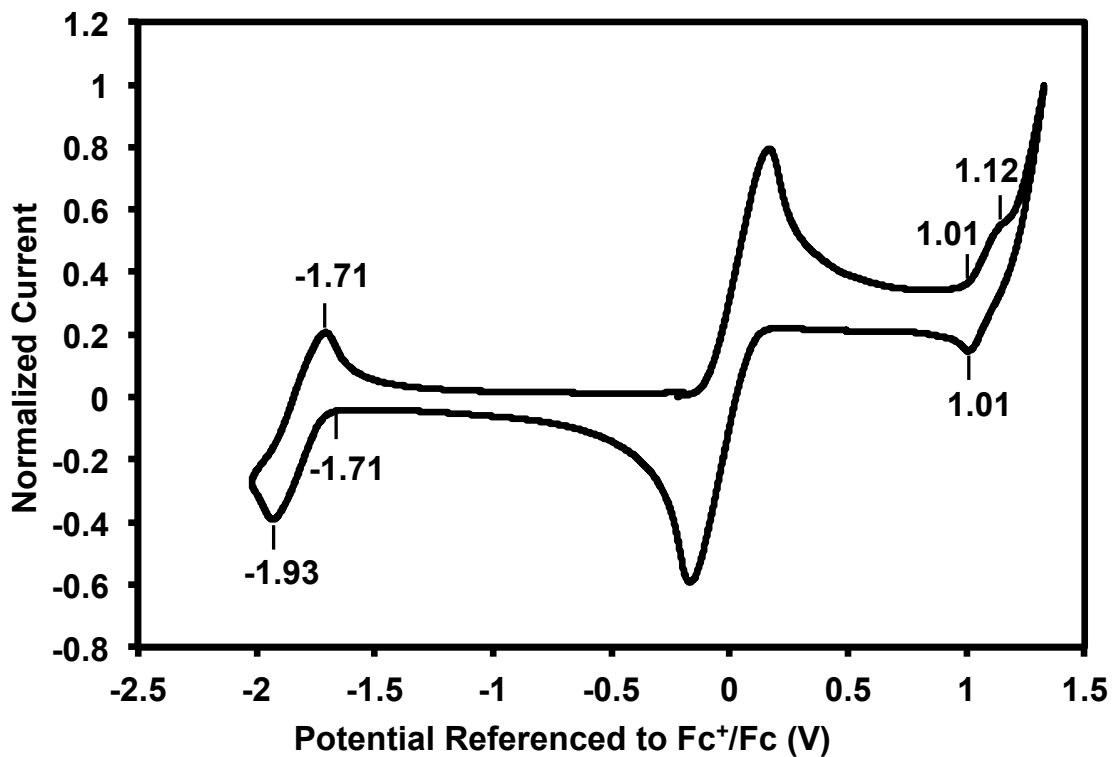


Figure S18: Cyclic voltammogram of 1.

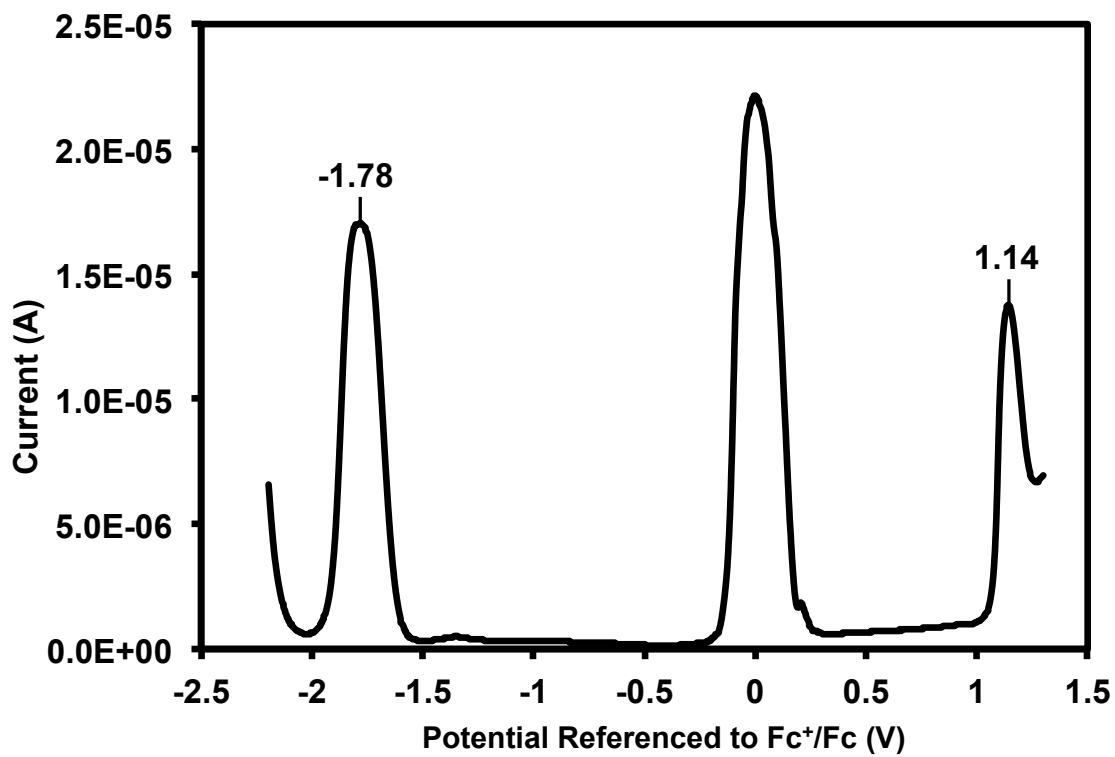


Figure S19: Differential pulse voltammogram of 1.

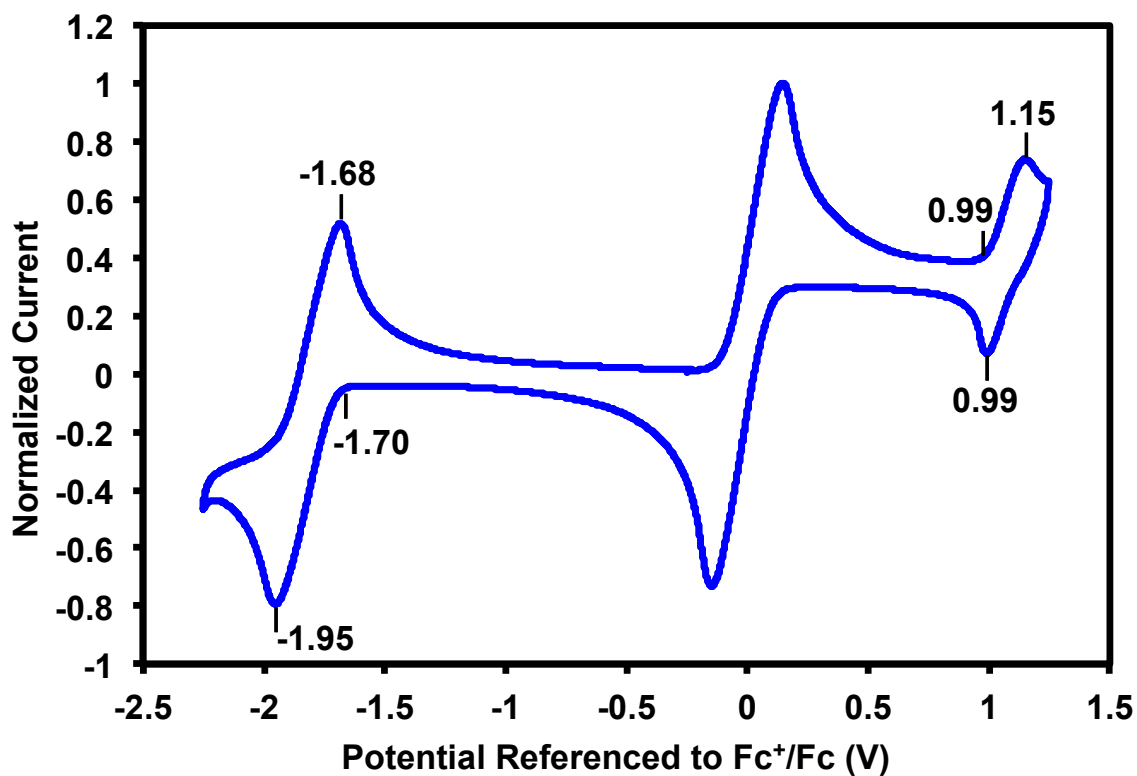


Figure S20: Cyclic voltammogram of 2.

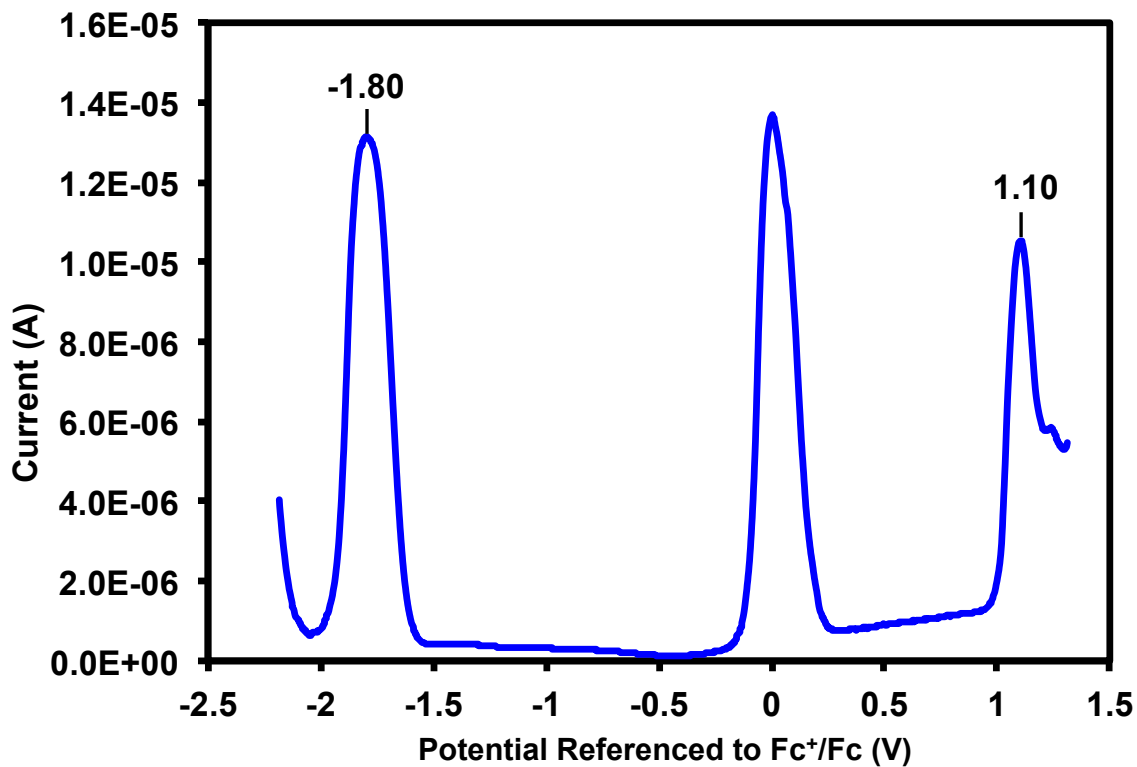


Figure S21: Differential pulse voltammogram of 2.

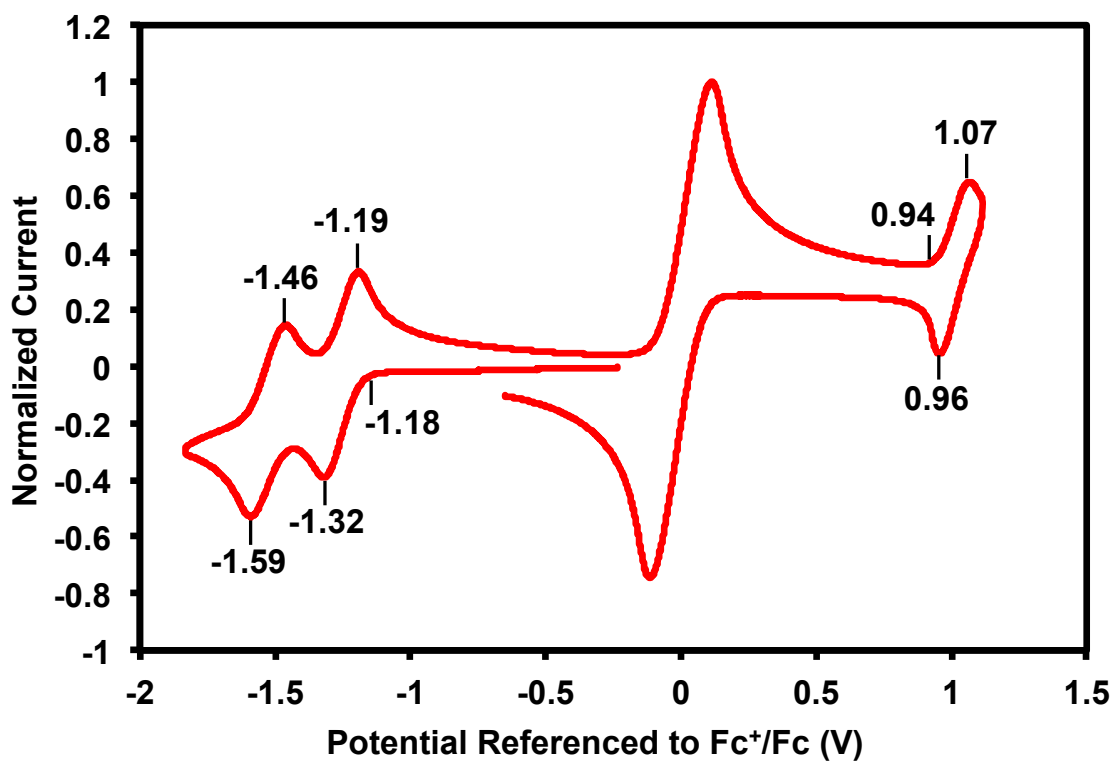


Figure S22: Cyclic voltammogram of 3.

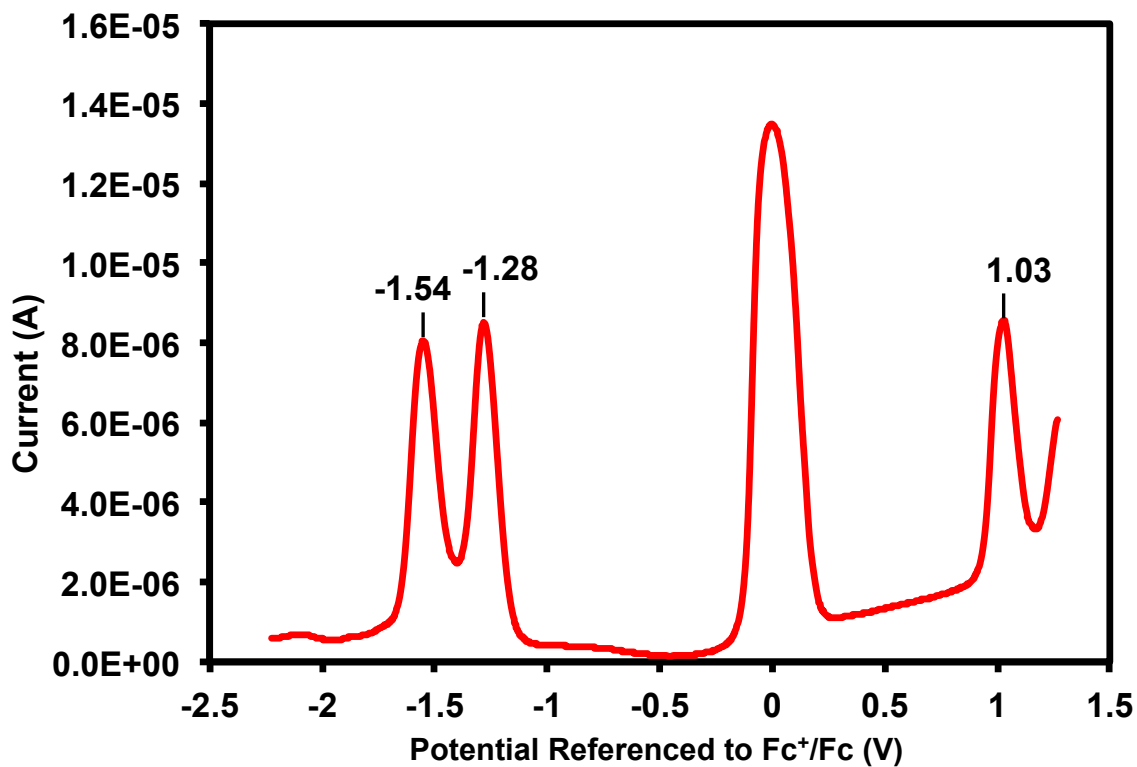


Figure S23: Differential pulse voltammogram of 3.

Table S2: Summary of electronic properties for **1**, **2**, and **3**.

	1	2	3
E _{Ox} Onset (V)	1.00	0.99	0.94
E _{1/2} Ox (V)	1.06	1.07	1.01
E _{Red} Onset (V)	-1.71	-1.70	-1.18
E _{1/2} Red (V)	-1.82	-1.82	-1.26, -1.53
HOMO (eV) ^a	-5.81	-5.79	-5.74
LUMO (eV) ^a	-3.09	-3.10	-3.62
E _g (eV)	2.72	2.69	2.12

^aEnergy values were calculated by (Onset V + 4.8) where 4.8 eV is HOMO of ferrocene.¹

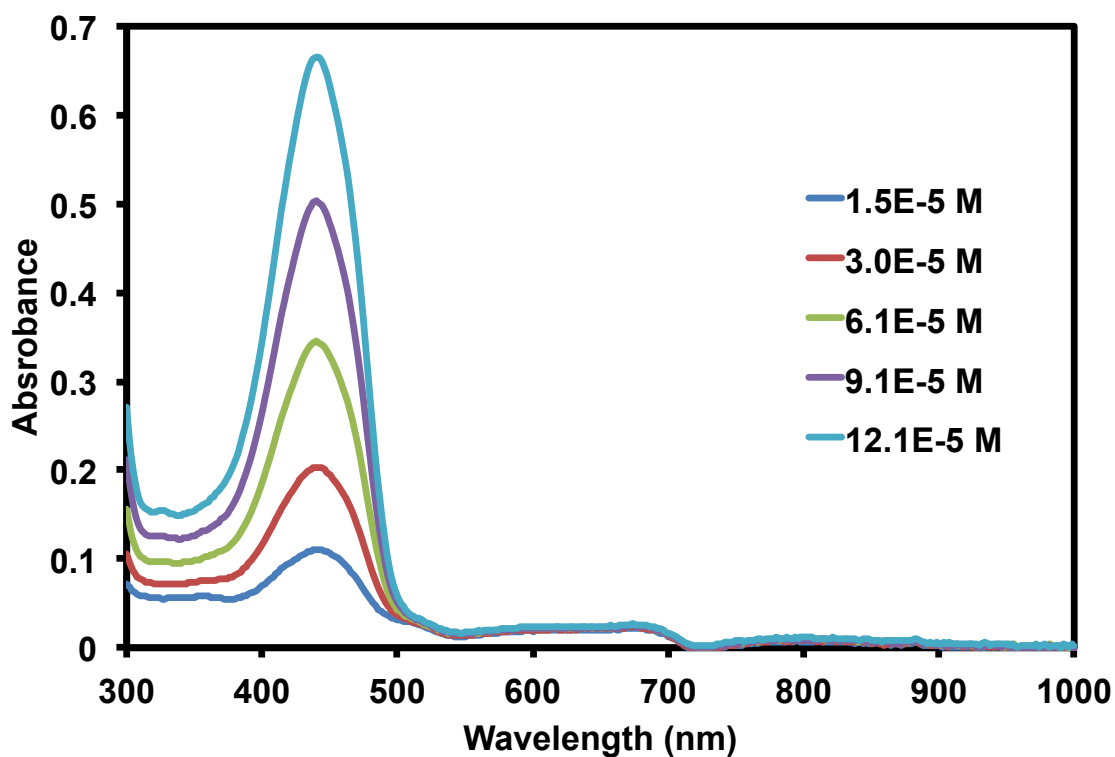


Figure S24: Solution absorption spectra for **1**.

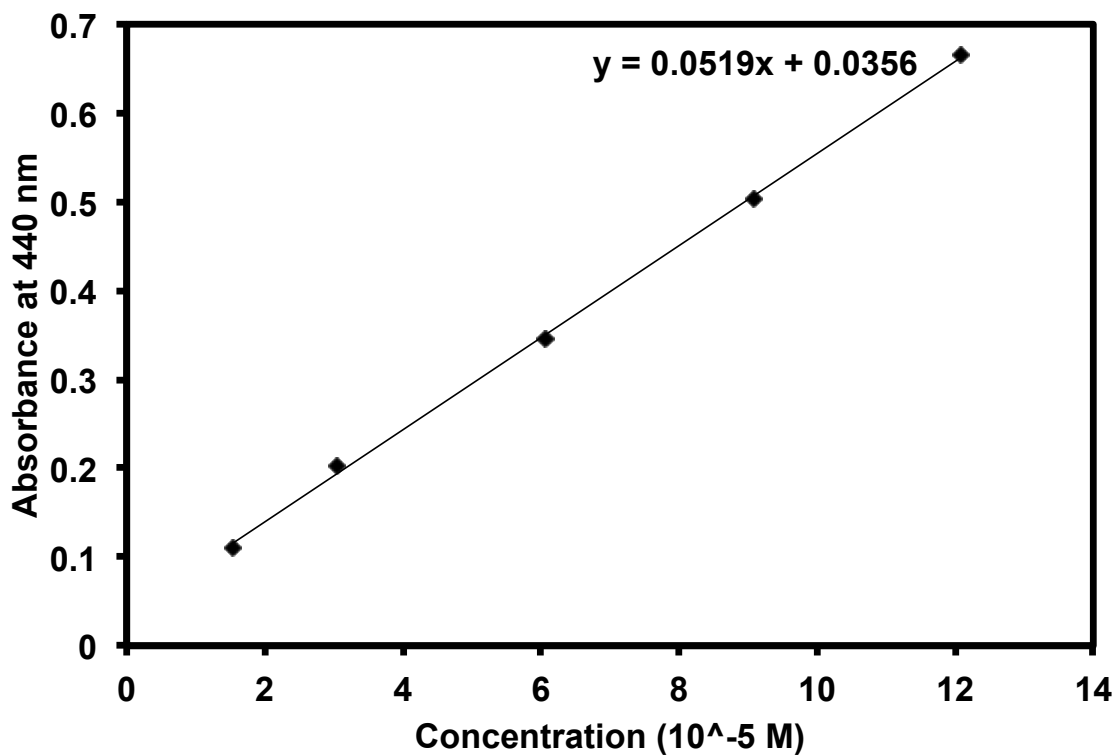


Figure S25: Absorbance versus concentration profile for 1.

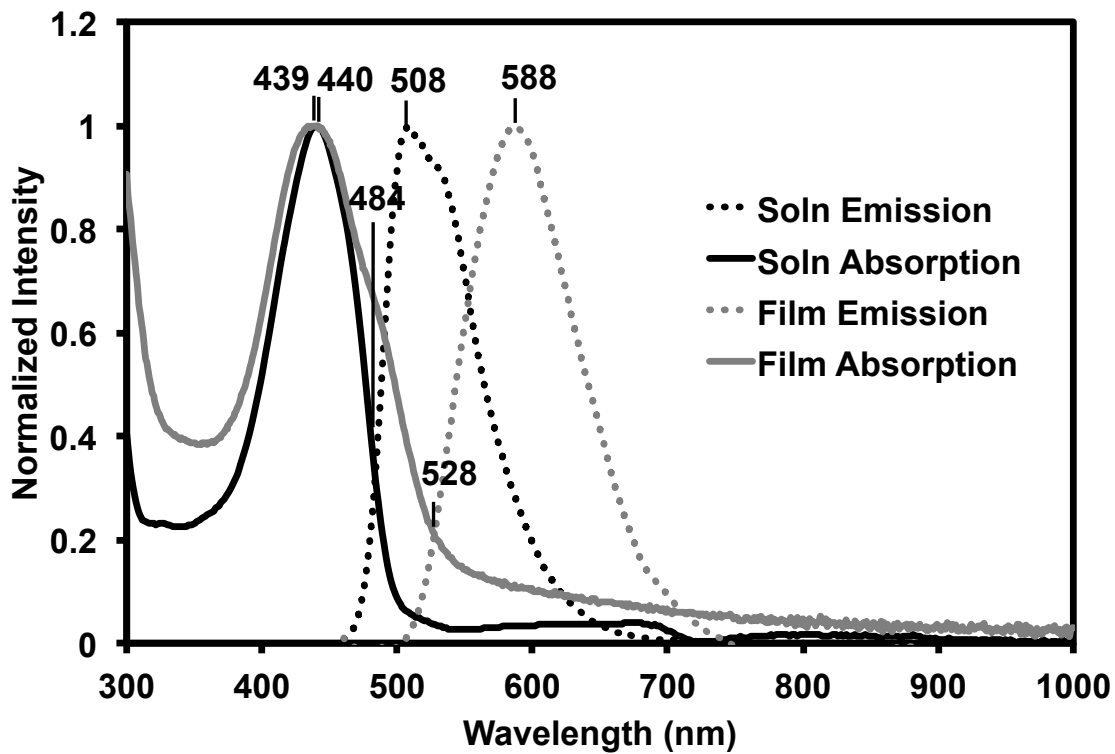


Figure S26: Solution and thin-film absorption and emission spectra for 1.

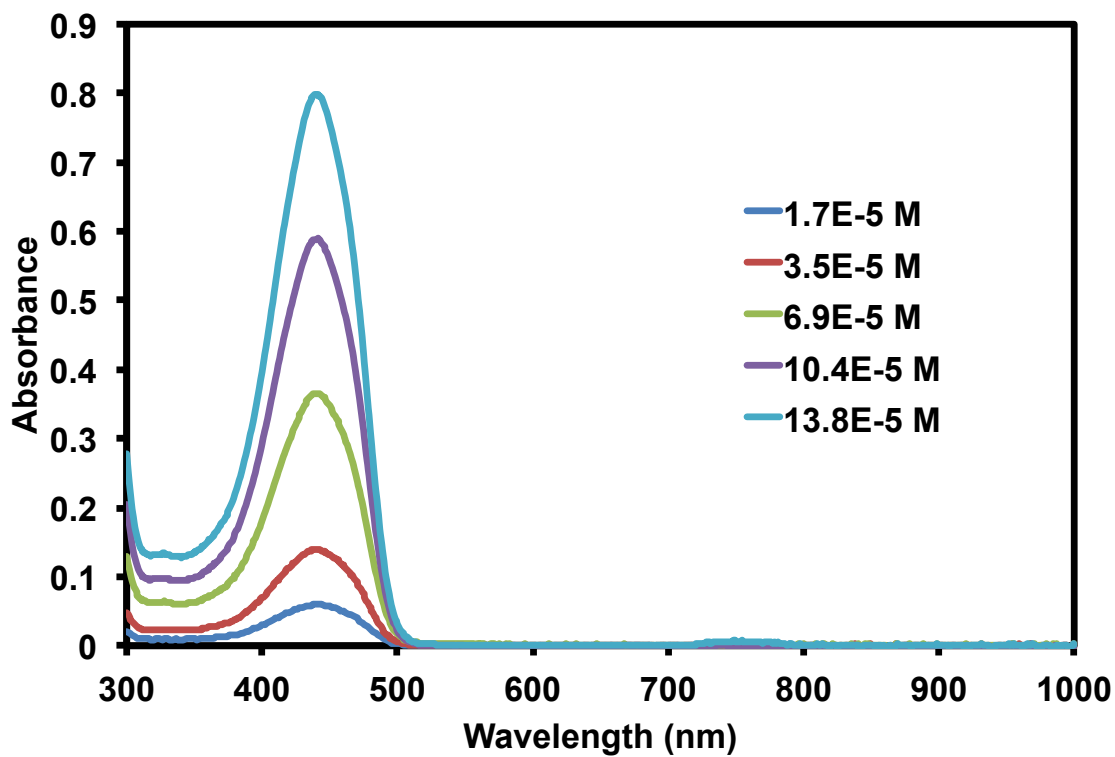


Figure S27: Solution absorption spectra for 2.

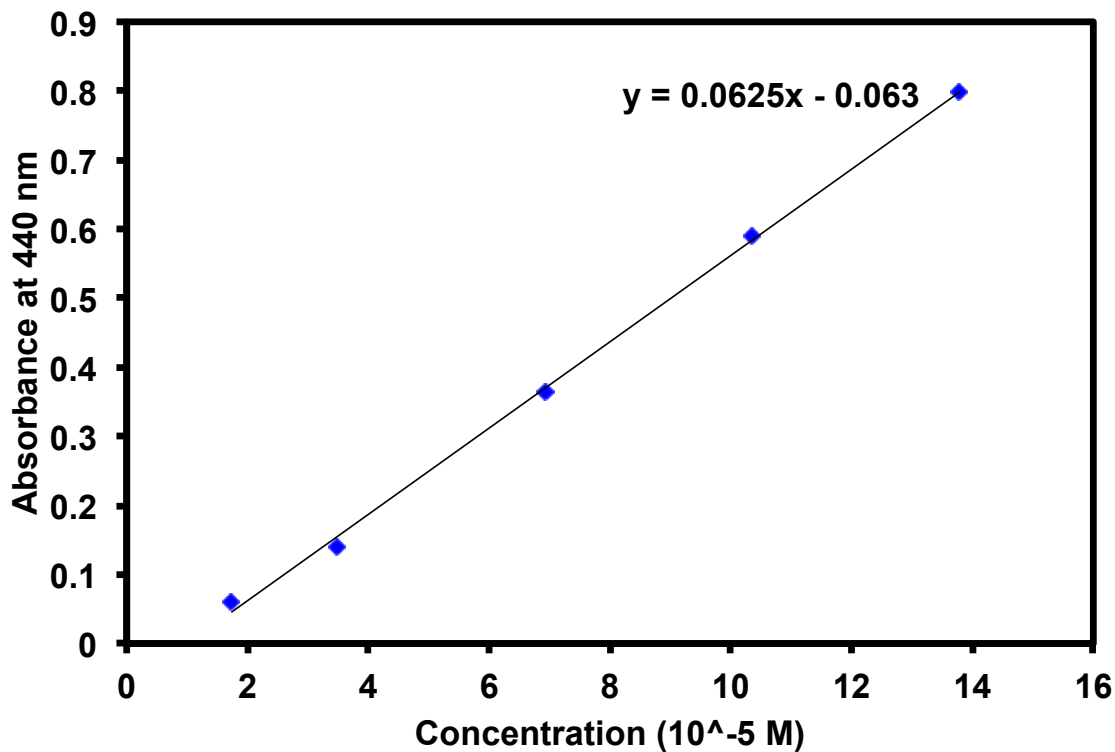


Figure S28: Absorbance versus concentration profile for 2.

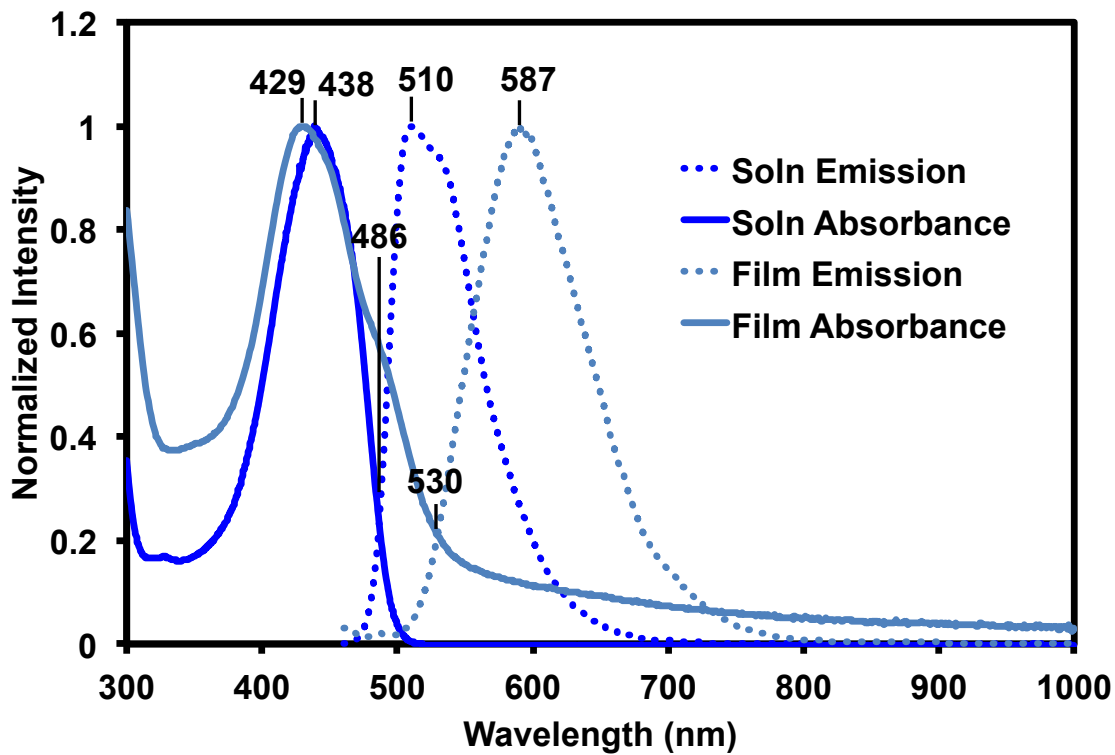


Figure S29: Solution and thin-film absorption and emission spectra for 2.

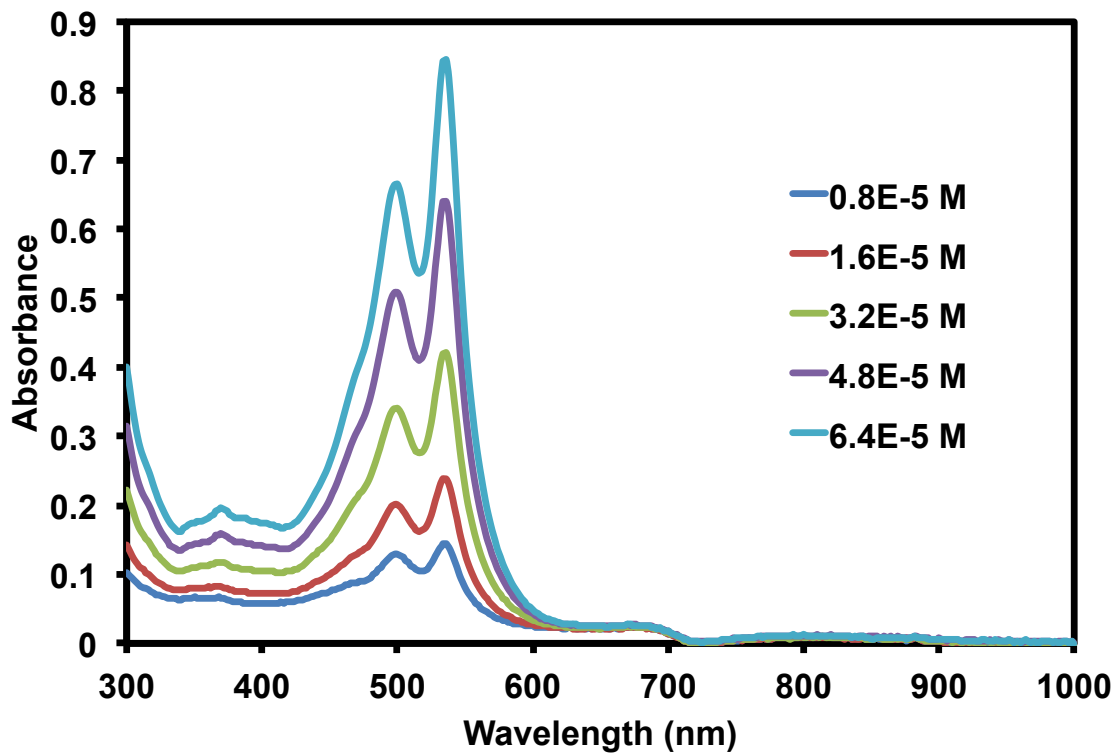


Figure S30: Solution absorption spectra for 3.

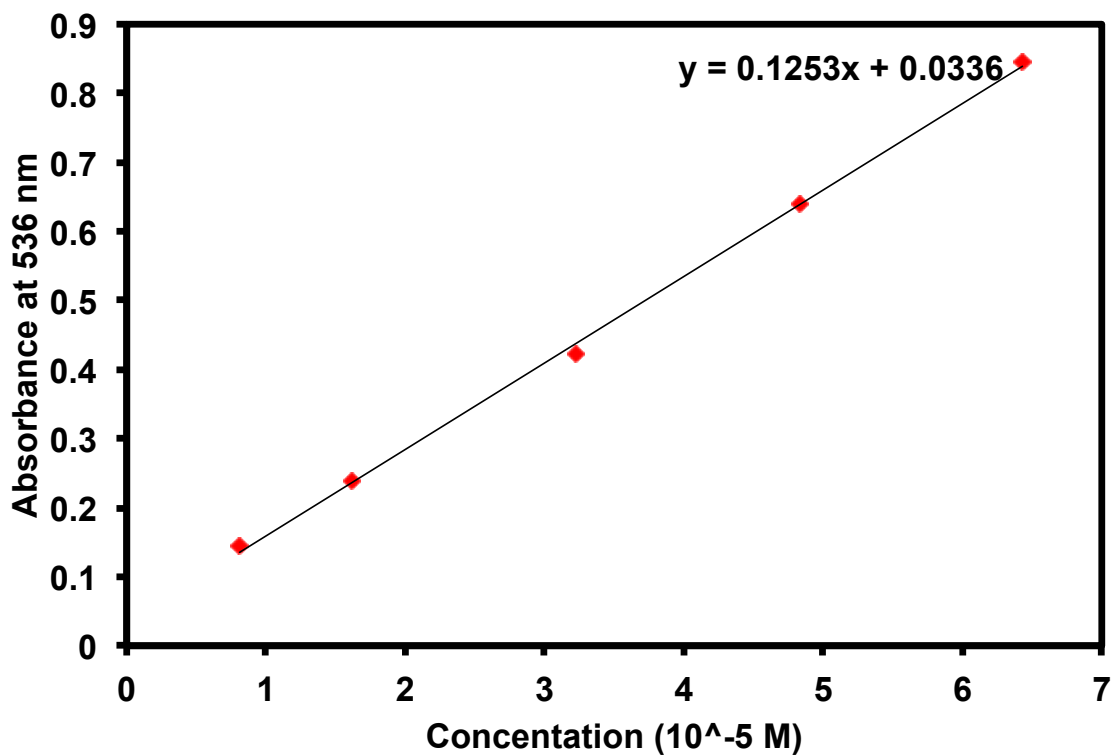


Figure S31: Absorbance versus concentration profile for 3.

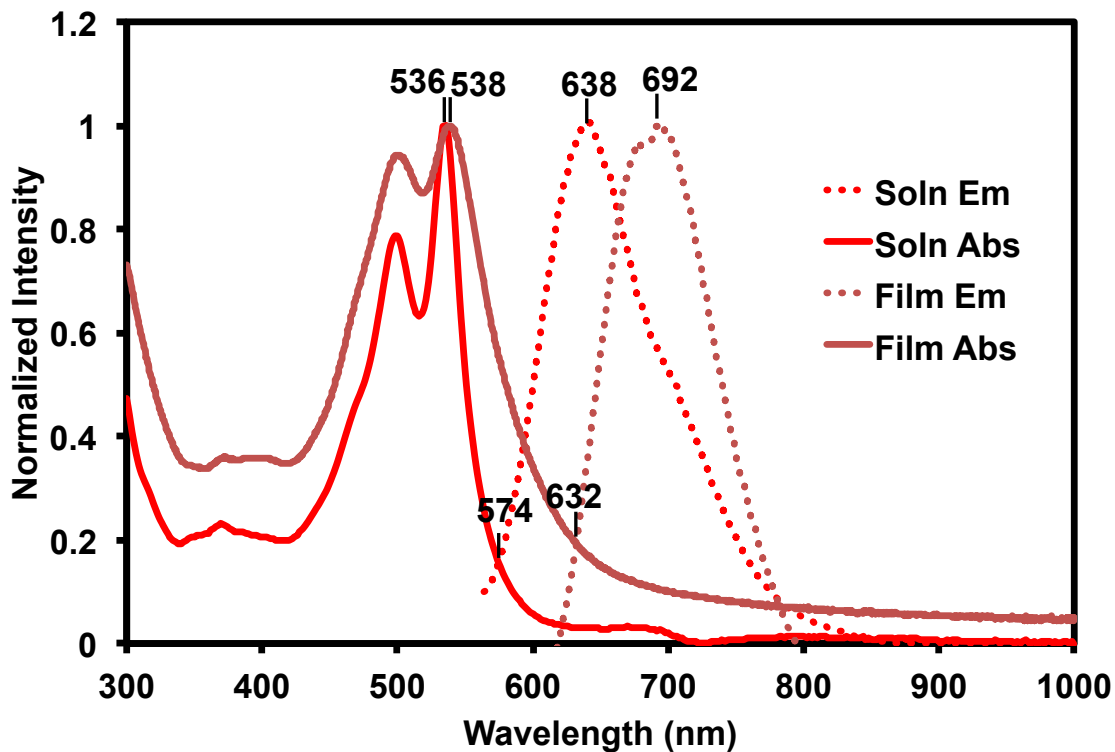


Figure S32: Solution and thin-film absorption and emission spectra for 3.

Table S3: Summary of optical properties for **1**, **2**, and **3**.

	1	2	3
Solution Absorbance Max (nm)	440	438	536
Solution Emission Max (nm)	508	510	638
Solution Optical E _g (eV) ^a	2.56	2.55	2.16
Solution Stokes Shift (eV) ^b	0.38	0.40	0.37
Molar Absorptivity (L mol ⁻¹ cm ⁻¹)	25939.31	31240.56	62633.81
Thin film Absorbance Max (nm)	439	429	538
Thin film Emission Max (nm)	588	588	692
Thin film Optical E _g (eV) ^a	2.35	2.34	1.96
Thin film Stokes Shift (eV) ^b	0.72	0.78	0.51
Excitation Wavelength (nm)	440	440	536

^aOptical band gaps were calculated from the wavelength intercept of absorption and emission profiles where ($E_{\lambda_{\text{int}}} = h \cdot c / \lambda_{\text{int}}$; h = Planck's Constant, c = speed of light).

^bStokes Shifts were calculated by ($E_{\lambda_{\text{abs}}} - E_{\lambda_{\text{ems}}}$) where ($E_{\lambda_{\text{max}}} = h \cdot c / \lambda_{\text{max}}$).

Thermal Properties Characterization (DSC/TGA)

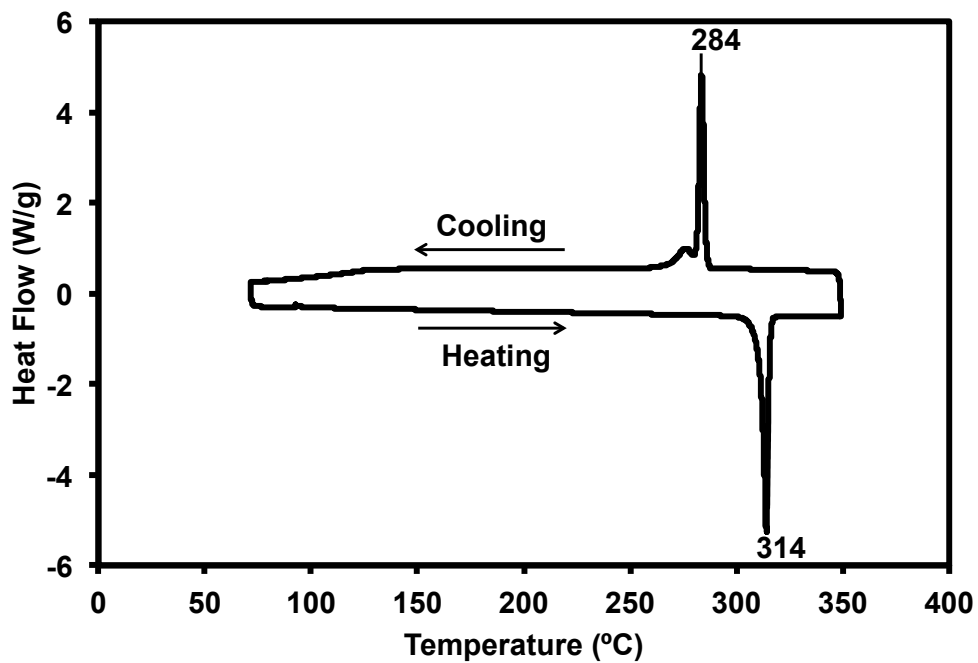


Figure S33: DSC profile for 1.

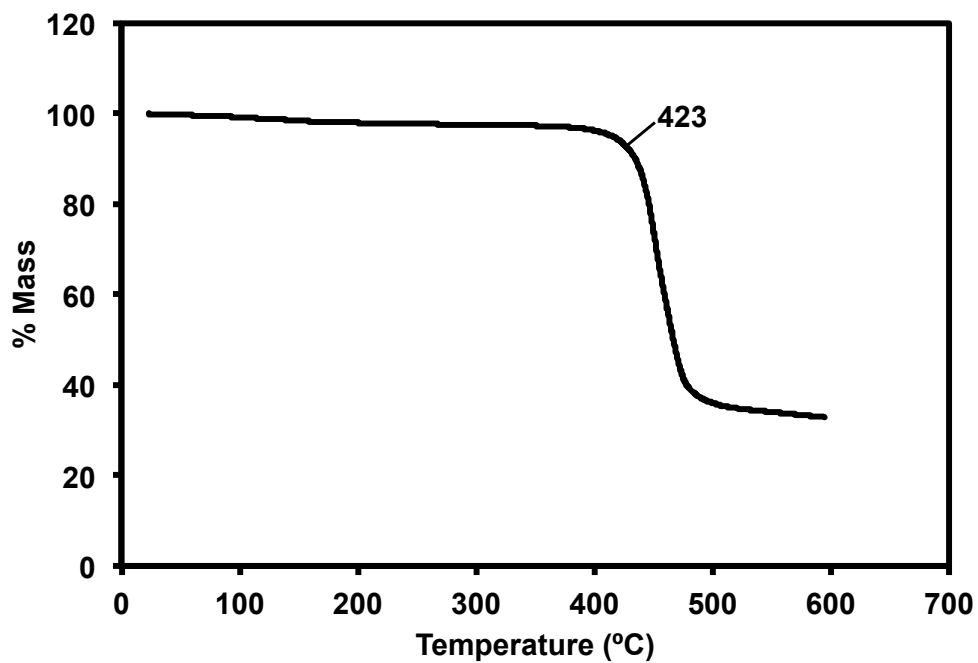


Figure S34: TGA profile for 1.

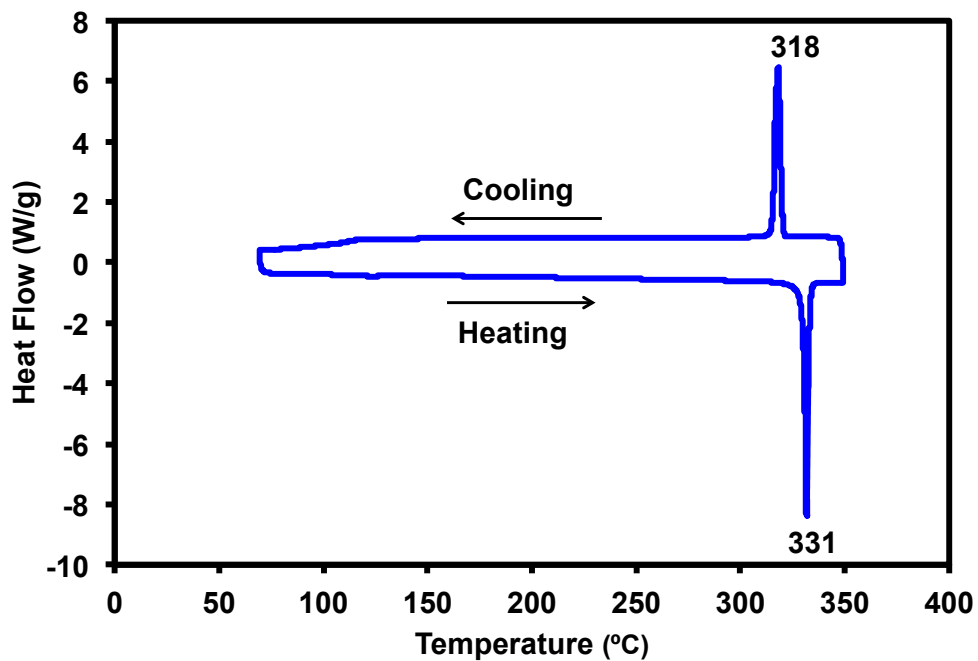


Figure S35: DSC profile for 2.

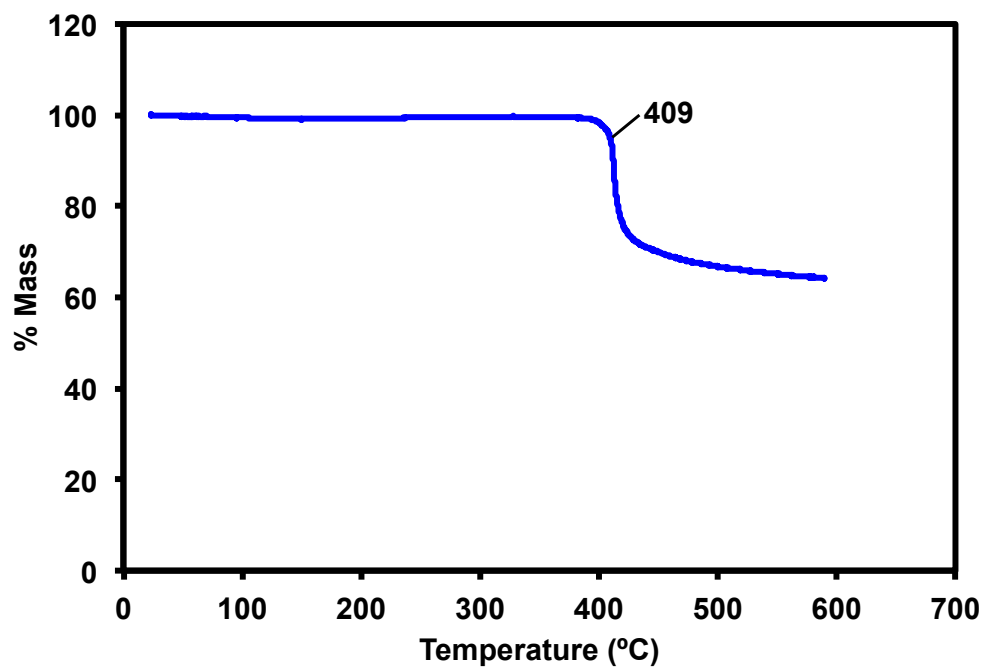


Figure S36: TGA profile for 2.

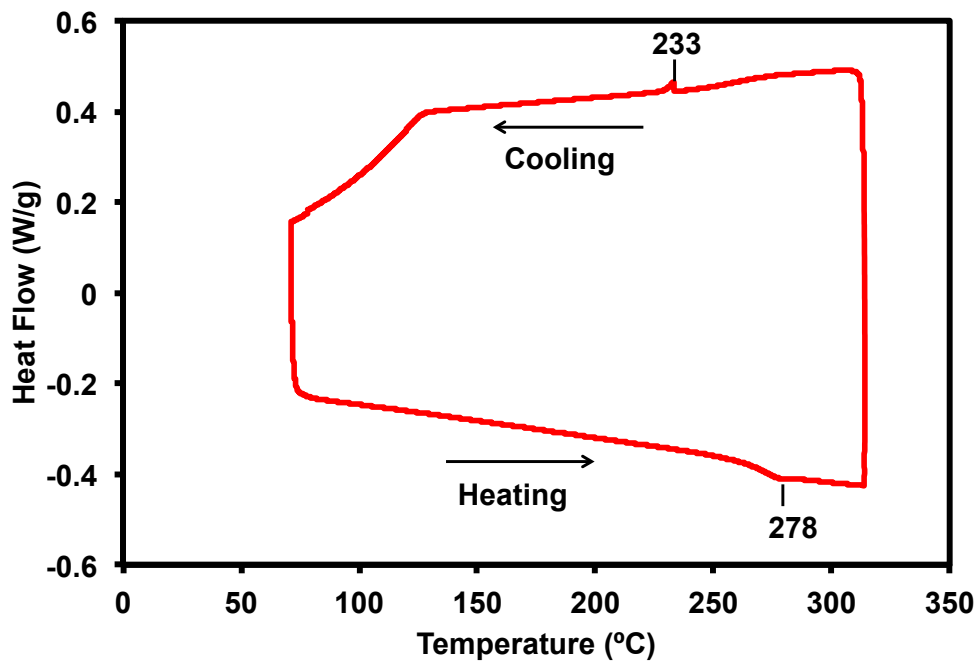


Figure S37: DSC profile for 3.

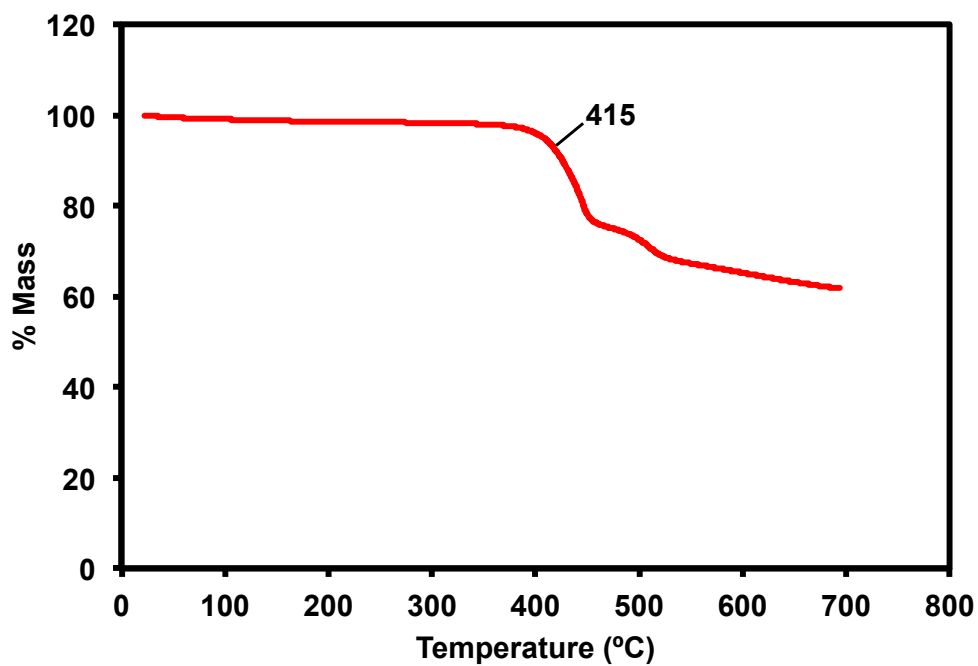


Figure S38: TGA profile for 3.

Table S4: Summary of thermal data for 1, 2, and 3.

	1	2	3
T_m (°C)	314	331	278
T_c (°C)	284	318	233
T_d (°C)	423	409	415

Density Functional Theory

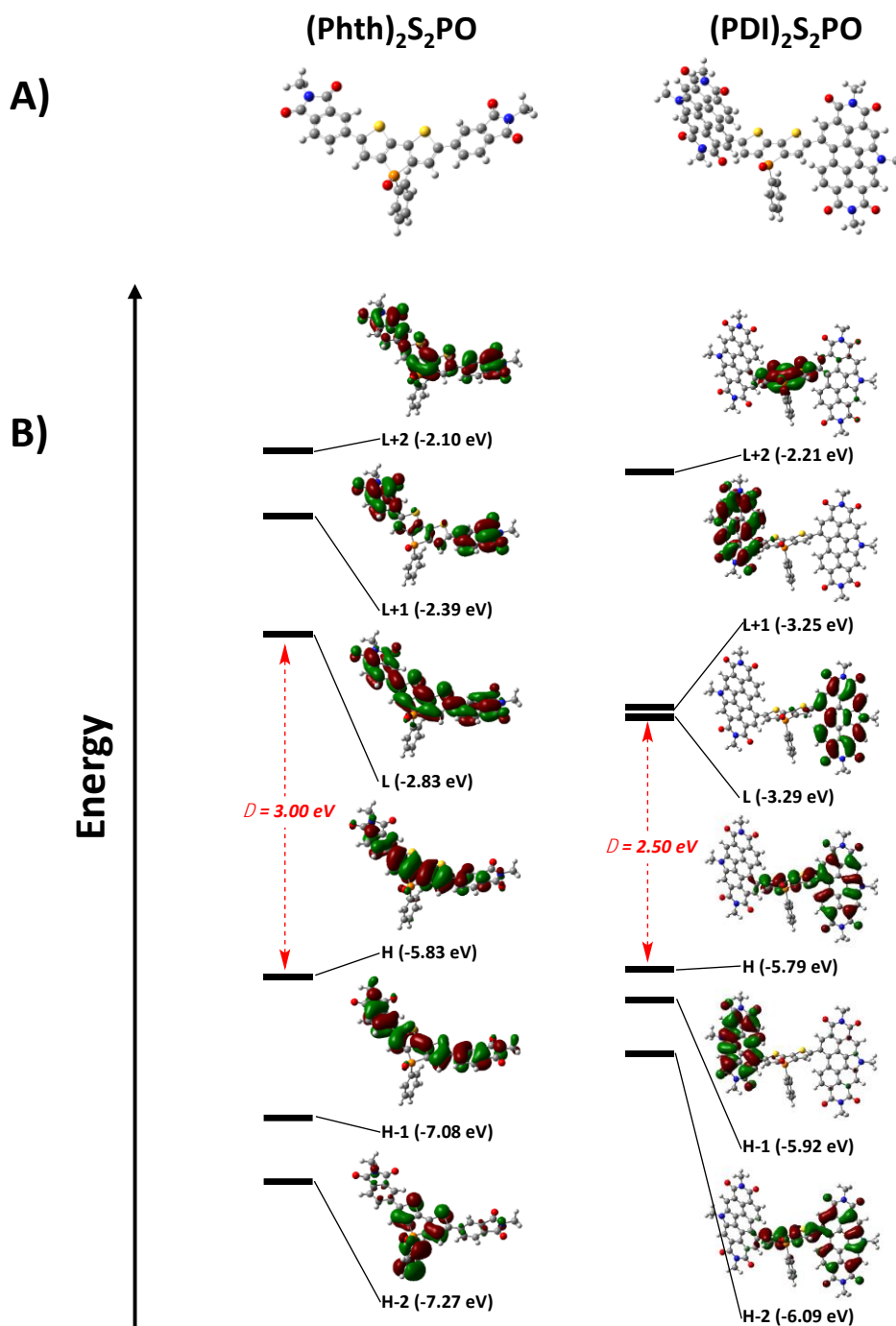


Figure S39: A) Optimized geometries for **2** and **3**. B) Calculated electronic energy levels and energy gaps for **2** and **3**. Calculations were done on Gaussian09,² and results were visualized using GausView05.³ All alkyl chains were replaced with a methyl group. The B3LYP⁴⁻⁶ level of theory with 6-31G(d,p)⁷⁻¹² basis set were used for the calculations. TD-SCF¹³ calculations were performed from the optimized geometry. The single point calculation was performed on this structure in order to generate molecular orbitals and electrostatic potential maps.

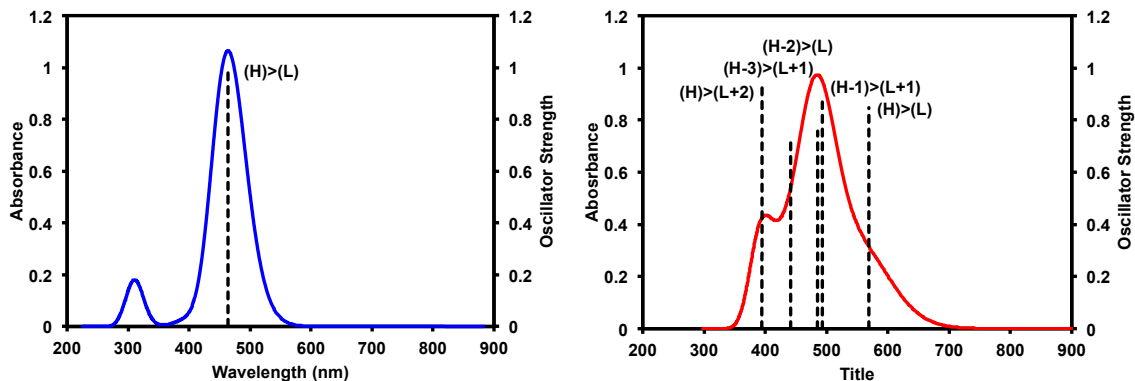


Figure S40: Calculated optical absorption profile for **2** and **3**.

Table S5: Summary of predicted optical transitions.

Compound	State	E_{opt} (eV)	λ (nm)	f	Composition
2	S_1	2.67	464	1.063	H \rightarrow L (99%)
3	S_1	2.18	569	0.243	H \rightarrow L (85%) H-2 \rightarrow L (12%) H \rightarrow L+1 (3%)
	S_4	2.51	493	0.265	H-1 \rightarrow L+1 (87%) H-2 \rightarrow L (7%) H-2 \rightarrow L+1 (2%)
	S_5	2.55	485	0.610	H-2 \rightarrow L (76%) H \rightarrow L (10%) H-1 \rightarrow L+1 (9%)
	S_7	2.81	441	0.258	H-3 \rightarrow L+1 (72%) H-4 \rightarrow L (21%)
	S_{11}	3.14	395	0.392	H \rightarrow L+2 (93%)

Organic Solar Cells

Devices were fabricated using ITO-coated glass substrates cleaned by sequentially ultra-sonicating detergent and de-ionized water, acetone, and isopropanol followed by exposure to UV/ozone for 30 minutes. ZnO was subsequently deposited as a sol-gel precursor solution in air following the method of Sun *et al.*¹⁸ The room temperature solution was filtered and spin-cast at a speed of 4000 rpm and then annealed at 200 °C in air for 15 min.

Active layer solutions of **PBDB-T** (Brilliant Matters, PCE12, $M_w = 154$ kg/mol and $M_n = 76$ kg/mol, batch no BM3-009-6), **PDTT-BOBT**¹⁹ or **PTB7-Th** (Cal-os Organic Semiconductors, PCE10, $M_n > 25$ kg/mol, Cat. No DP0201, lot no C-03) and **3** were prepared in air with a total concentration of 10 mg/mL (or otherwise indicated) in CHCl_3 or *o*-dichlorobenzene (*o*-DCB) with or without a 0.5% (v/v) 1,8-diiodooctane (DIO) additive. Additional devices were cast using different concentrations of DIO (up to 5% (v/v)) or 1% (v/v) of diphenyl ether (DPE) or 1% (v/v) of 1-chloronaphthalene (CN). Solutions were stirred overnight at room temperature and heated for 4 h at 40 °C for CHCl_3 solutions and 4 h at 80 °C for *o*-DCB solutions. Active layer materials were combined in a 1:1 weight ratio (or otherwise indicated) and cast at room temperature in air at a speed of 1500 rpm (or otherwise indicated) for 60 seconds. Thermal annealing was done for 5 min at 100 °C or 200 °C when indicated.

The substrates with the cast active layers were kept in an N_2 atmosphere glovebox overnight before evaporating MoO_3 and Ag. The evaporation of 10 nm of MoO_3 followed by 100 nm of Ag were thermally deposited under vacuum (1×10^{-6} Torr). The active areas of resulting devices were 0.09 cm^2 . Statistics listed below for each device were tabulated from at least two substrates containing two devices each for a total of four devices.

Table S6: Organic solar cell data. Best results are highlighted in bold. Averages are in italics.

Materials	Ratio	Solvent	Parameters	V_{oc} (V)	J_{sc} (mA/cm ²)	FF (%)	PCE (%)
PBDB-T/3	1:1	CF	As cast	1.10	1.69	25.1	0.47
				1.11	1.79	25.2	0.50
				1.10	1.83	25.2	0.51
				1.11	1.92	25.3	0.54
				<i>1.10</i>	<i>1.81</i>	<i>25.2</i>	<i>0.50</i>
	0.5% DIO	1.09	0.97	25.5	0.27		
		1.08	0.96	25.3	0.26		
		1.10	1.98	25.9	0.57		
		1.11	2.01	25.8	0.58		
		<i>1.10</i>	<i>1.48</i>	<i>25.6</i>	<i>0.42</i>		
PBDB-T/3	1:1	<i>o</i> -DCB	As cast	1.11	3.82	28.2	1.19
				1.10	3.64	29.4	1.17
				1.10	3.77	29.8	1.24
				1.08	3.67	30.3	1.20
				<i>1.10</i>	<i>3.73</i>	<i>29.4</i>	<i>1.20</i>
	0.5% DIO	1.03	3.26	29.4	0.95		
		1.11	3.82	28.2	1.19		
		1.01	3.57	28.9	1.04		
		1.11	3.63	29.8	1.20		
		<i>1.07</i>	<i>3.57</i>	<i>29.1</i>	<i>1.10</i>		

PDTT- BOBT/3	1:1	CF	As cast	0.92	3.95	27.9	1.01
				1.00	3.43	30.0	1.02
				0.99	3.06	29.4	0.89
				1.00	3.37	29.4	0.99
				<i>0.98</i>	<i>3.45</i>	<i>29.2</i>	<i>0.98</i>
			0.5% DIO	1.00	6.28	34.4	2.16
				1.00	5.96	34.7	2.06
				0.99	5.83	34.9	2.02
				1.01	6.44	34.8	2.26
				<i>1.00</i>	<i>6.13</i>	<i>34.7</i>	<i>2.12</i>
PDTT- BOBT/3	1:1	<i>o</i> -DCB	As cast	0.96	2.16	44.1	0.91
				0.99	2.53	43.8	1.10
				0.97	2.51	41.5	1.01
				0.86	2.80	39.5	0.95
				<i>0.95</i>	<i>2.50</i>	<i>42.2</i>	<i>0.99</i>
			0.5% DIO	0.90	2.26	37.3	0.75
				1.01	2.69	45.3	1.23
				0.93	2.15	37.8	0.75
				0.95	2.64	37.1	0.93
				<i>0.94</i>	<i>2.43</i>	<i>39.4</i>	<i>0.92</i>
PTB7-Th/3	1:1	CF	As cast	1.00	3.54	28.4	1.01
				0.98	3.76	28.8	1.06
				0.99	3.94	28.5	1.11
				0.96	3.38	27.8	0.90
				<i>0.98</i>	<i>3.66</i>	<i>28.4</i>	<i>1.02</i>
			0.5% DIO	1.03	3.04	25.3	0.79
				1.02	2.60	25.8	0.68
				0.98	2.94	27.9	0.81
				0.99	2.89	27.5	0.79
				<i>1.01</i>	<i>2.87</i>	<i>26.6</i>	<i>0.77</i>
PTB7-Th/3	1:1	<i>o</i> -DCB	As cast	1.00	5.11	37.1	1.89
				0.98	5.76	34.4	1.94
				0.99	4.80	36.9	1.76
				1.00	5.70	36.0	2.05
				<i>0.99</i>	<i>5.34</i>	<i>36.1</i>	<i>1.91</i>
			0.5% DIO	1.01	4.84	35.4	1.73
				1.02	5.50	35.9	2.01
				0.99	4.62	39.1	1.78
				0.99	5.39	37.8	2.03
				<i>1.00</i>	<i>5.09</i>	<i>37.0</i>	<i>1.89</i>

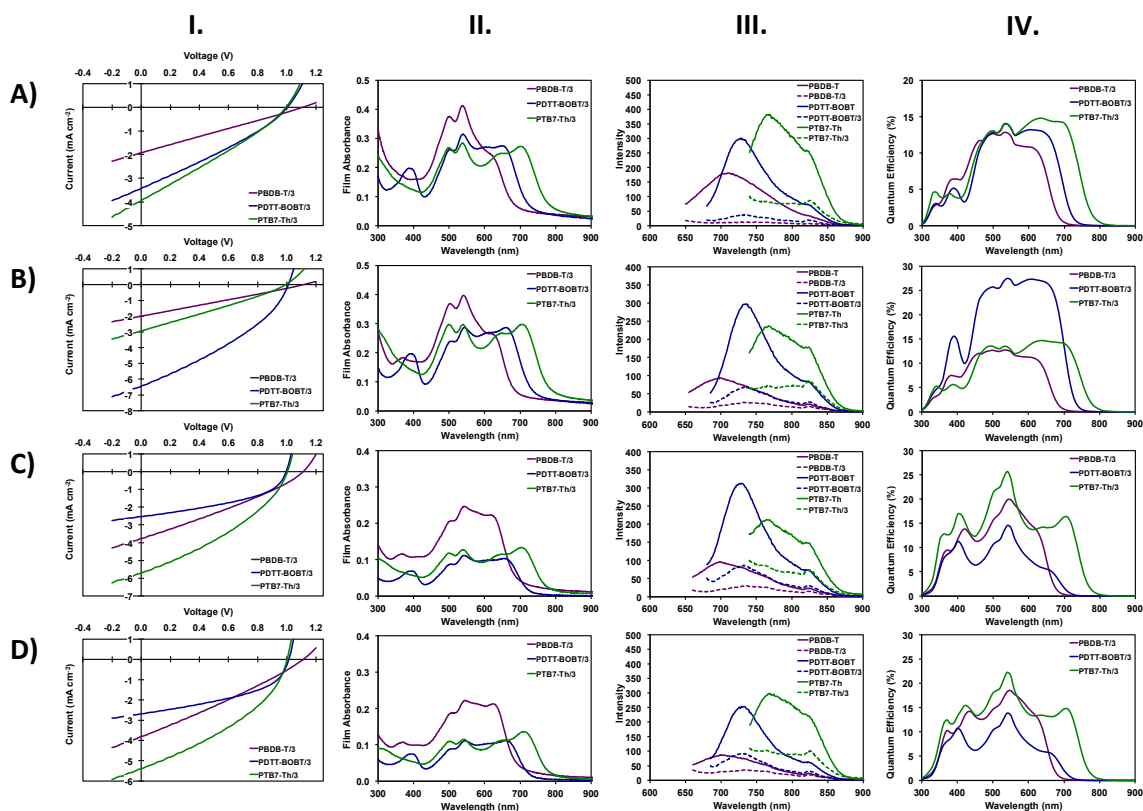


Figure S41: I. JV curves, II. UV-vis spectra, III. photoluminescence spectra, and IV. EQE profiles of blends for A) as cast in chloroform, B) 0.5% DIO in chloroform, C) as cast in *o*-dichlorobenzene, and D) 0.5% DIO in *o*-dichlorobenzene.

Table S7: Photoluminescence spectra excitation wavelengths for active layer blends.

Blend	Conditions	Excitation Wavelength (nm)
PBDB-T/3	As cast, chloroform	618
PDDT-BOBT/3	As cast, chloroform	658
PTB7-Th/3	As cast, chloroform	705
PBDB-T/3	0.5% DIO, chloroform	623
PDDT-BOBT/3	0.5% DIO, chloroform	662
PTB7-Th/3	0.5% DIO, chloroform	705
PBDB-T/3	As cast, <i>o</i> -dichlorobenzene	625
PDDT-BOBT/3	As cast, <i>o</i> -dichlorobenzene	658
PTB7-Th/3	As cast, <i>o</i> -dichlorobenzene	705
PBDB-T/3	0.5% DIO, <i>o</i> -dichlorobenzene	625
PDDT-BOBT/3	0.5% DIO, <i>o</i> -dichlorobenzene	662
PTB7-Th/3	0.5% DIO, <i>o</i> -dichlorobenzene	705

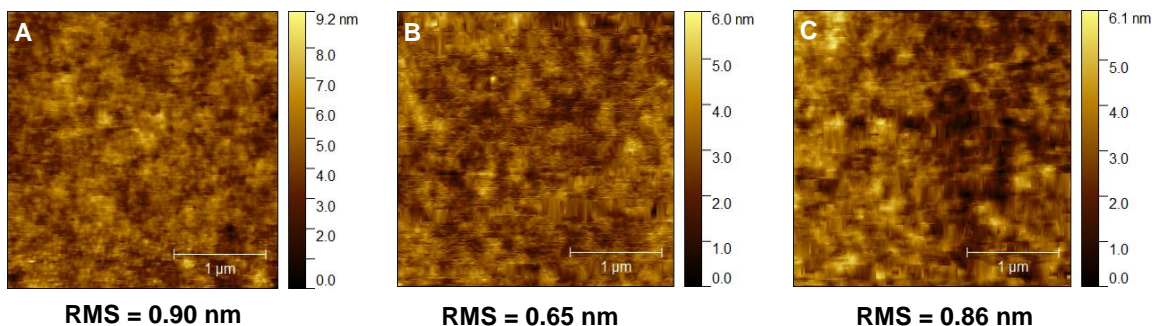


Figure S42: AFM images of organic solar cell devices for A) PBDB-T/3, B) PDTT-BOBT/3, and C) PTB7-Th/3, as cast from *o*-DCB.

Table S8: Organic solar cell data for the PBDB-T/3 blend cast from *o*-DCB. Best results are highlighted in bold. Averages are in italics.

Ratio	Parameters	V_{oc} (V)	J_{sc} (mA/cm ²)	FF (%)	PCE (%)
1:1	15 mg/mL, as cast	1.09	2.35	27.8	0.71
		1.09	2.37	27.7	0.72
		<i>1.09</i>	<i>2.36</i>	<i>27.78</i>	<i>0.71</i>
1:1	15 mg/mL, 1000 rpm, as cast	1.06	1.10	27.8	0.32
		1.06	1.14	27.8	0.34
		<i>1.06</i>	<i>1.12</i>	<i>27.8</i>	<i>0.33</i>
1:1	Thermal annealing, 5 min @ 100 °C	1.07	3.68	28.3	1.11
		0.99	3.00	27.1	0.81
		<i>1.03</i>	<i>3.34</i>	<i>27.7</i>	<i>0.96</i>
1:1	Thermal annealing, 5 min @ 200 °C	1.08	3.38	30.3	1.11
		1.07	3.02	29.4	0.95
		<i>1.07</i>	<i>3.20</i>	<i>29.9</i>	<i>1.03</i>
2:3	As cast	0.98	2.53	25.95	0.64
		1.04	2.47	25.58	0.66
		<i>1.01</i>	<i>2.50</i>	<i>25.77</i>	<i>0.65</i>
3:2	As cast	1.03	3.04	30.44	0.96
		1.09	3.23	30.00	1.06
		<i>1.06</i>	<i>3.14</i>	<i>30.22</i>	<i>1.01</i>
7:3	As cast	0.66	2.20	26.3	0.38
		0.62	2.49	27.2	0.42
		<i>0.64</i>	<i>2.34</i>	<i>26.71</i>	<i>0.40</i>
3:7	As cast	0.77	2.74	28.5	0.60
		0.78	3.29	28.8	0.74
		<i>0.78</i>	<i>3.02</i>	<i>28.63</i>	<i>0.67</i>
1:1	1% DIO	1.11	3.37	28.9	1.08
		1.11	3.28	29.3	1.07
		<i>1.11</i>	<i>3.32</i>	<i>29.1</i>	<i>1.07</i>
1:1	3% DIO	1.08	2.81	29.2	0.89
		1.09	2.72	29.3	0.87
		<i>1.08</i>	<i>2.76</i>	<i>29.3</i>	<i>0.88</i>
1:1	5% DIO	1.09	2.81	29.0	0.89
		1.09	3.01	29.2	0.96
		<i>1.09</i>	<i>2.91</i>	<i>29.1</i>	<i>0.92</i>
1:1	1% DPE	1.11	3.20	26.9	0.96
		1.12	3.29	26.8	0.99
		<i>1.12</i>	<i>3.24</i>	<i>26.9</i>	<i>0.97</i>

1:1	1% CN	1.09	4.54	34.3	1.69
		1.09	4.91	33.6	1.79
		1.04	4.37	31.7	1.44
		1.07	4.57	33.2	1.62
		<i>1.07</i>	<i>4.60</i>	<i>33.2</i>	<i>1.64</i>

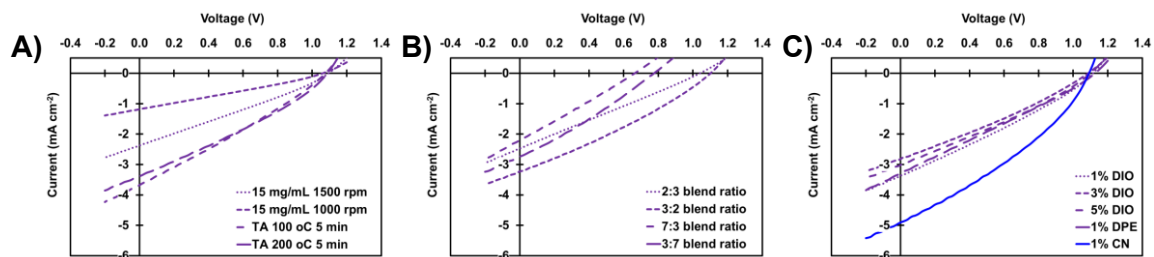


Figure S43: Additional JV curves of PBDB-T/3 blends cast from *o*-DCB with A) different concentration, spin-coating speed, and thermal annealing; B) different donor/acceptor ratio; and C) containing different concentrations of additives.

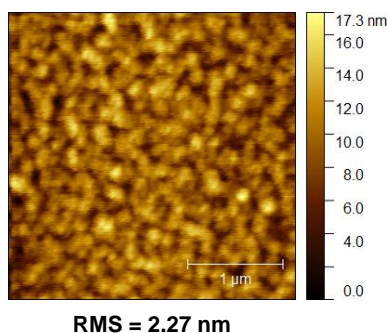


Figure S44: AFM images of organic solar cell device for PBDB-T/3 containing 1% (v/v) 1-chloronaphthalene, cast from *o*-DCB.

References

- (1) Pommerehne, J.; Vestweber, H.; Guss, W.; Mahrt, R. F.; Bäessler, H.; Porsch, M.; Daub, J. *Adv. Mater.* **1995**, *7* (6), 551–554.
- (2) Frisch, M.; Trucks, G.; Schlegel, H.; Scuseria, G.; Robb, M.; Cheeseman, J.; Scalmani, G.; Barone, V.; Mennucci, B.; Petersson, G.; Nakatsuji, H.; Caricato, M.; Li, X.; Hratchian, H.; Izmaylov, A.; Bloino, J.; Zheng, G.; Sonnenberg, J.; Hada, M.; Ehara, M.; Toyota, K.; Fukuda, R.; Hasegawa, J.; Ishida, M.; Nakajima, T.; Honda, Y.; Kitao, O.; Nakai, H.; Vreven, T.; Montgomery, J.; Peralta, J.; Ogliaro, F.; Bearpark, M.; Heyd, J.; Brothers, E.; Kudin, K.; Staroverov, V.; Kobayashi, R.; Normand, J.; Raghavachari, K.; Rendell, A.; Burant, J.; Iyengar, S.; Tomasi, J.; Cossi, M.; Rega, N.; Millam, J.; Klene, M.; Knox, J.; Cross, J.; Bakken, V.; Adamo, C.; Jaramillo, J.; Gomperts, R.; Stratmann, R.; Yazyev, O.; Austin, A.; Cammi, R.; Pomelli, C.; Ochterski, J.; Martin, R.; Morokuma, K.; Zakrzewski, V.; Voth, G.; Salvador, P.; Dannenberg, J.; Dapprich, S.; Daniels, A.; Farkas; Foresman, J.; Ortiz, J.; Cioslowski, J.; Fox, D. *Gaussian 09 Revis. B01 Gaussian Inc Wallingford CT* **2009**.
- (3) *GaussView Version 5*.

- (4) Becke, A. D. *Phys. Rev. A* **1988**, 38 (6), 3098–3100.
- (5) Lee, C.; Yang, W.; Parr, R. G. *Phys. Rev. B* **1988**, 37 (2), 785–789.
- (6) Miehlich, B.; Savin, A.; Stoll, H.; Preuss, H. *Chem. Phys. Lett.* **1989**, 157 (3), 200–206.
- (7) Hehre, W. J.; Ditchfield, R.; Pople, J. A. *J. Chem. Phys.* **1972**, 56 (5), 2257–2261.
- (8) Hariharan, P. C.; Pople, J. A. *Theor. Chim. Acta* **1973**, 28 (3), 213–222.
- (9) Francl, M. M.; Pietro, W. J.; Hehre, W. J.; Binkley, J. S.; Gordon, M. S.; DeFrees, D. J.; Pople, J. A. *J. Chem. Phys.* **1982**, 77 (7), 3654–3665.
- (10) Binning, R. C.; Curtiss, L. A. *J. Comput. Chem.* **1990**, 11 (10), 1206–1216.
- (11) Rassolov, V. A.; Pople, J. A.; Ratner, M. A.; Windus, T. L. *J. Chem. Phys.* **1998**, 109 (4), 1223–1229.
- (12) Rassolov, V. A.; Ratner, M. A.; Pople, J. A.; Redfern, P. C.; Curtiss, L. A. *J. Comput. Chem.* **2001**, 22 (9), 976–984.
- (13) Bauernschmitt, R.; Ahlrichs, R. *Chem. Phys. Lett.* **1996**, 256 (4–5), 454–464.
- (14) Hendsbee, A. D.; Sun, J.-P.; Law, W. K.; Yan, H.; Hill, I. G.; Spasyuk, D. M.; Welch, G. C. *Chem. Mater.* **2016**, 28 (19), 7098–7109.
- (15) Sun, J.-P.; D. Hendsbee, A.; F. Eftaiha, A.; Macaulay, C.; R. Rutledge, L.; C. Welch, G.; G. Hill, I. *J. Mater. Chem. C* **2014**, 2 (14), 2612–2621.
- (16) Josse, P.; Labrunie, A.; Dalinot, C.; McAfee, S. M.; Dabos-Seignon, S.; Roncali, J.; Welch, G. C.; Blanchard, P.; Cabanetos, C. *Org. Electron.* **2016**, 37 (Supplement C), 479–484.
- (17) Baumgartner, T.; Neumann, T.; Wirges, B. *Angew. Chem. Int. Ed.* **2004**, 43 (45), 6197–6201.
- (18) Sun, Y.; Seo, J. H.; Takacs, C. J.; Seifert, J.; Heeger, A. J. *Adv. Mater.* **2011**, 23 (14), 1679–1683.
- (19) Kini, G. P.; Lee, S. K.; Shin, W. S.; Moon, S.-J.; Song, C. E.; Lee, J.-C. *J. Mater. Chem. A* **2016**, 4 (47), 18585–18597.